Investigation of a small width Heat-Sink with considerations for use with Thermo Electric Generators

Masters thesis

Lars Kuur

MASTER'S THESIS
within
THERMAL ENERGY AND PROCESS ENGINEERING

Department of Energy Technology
University of Aalborg, Denmark

May 31^{st} 2011

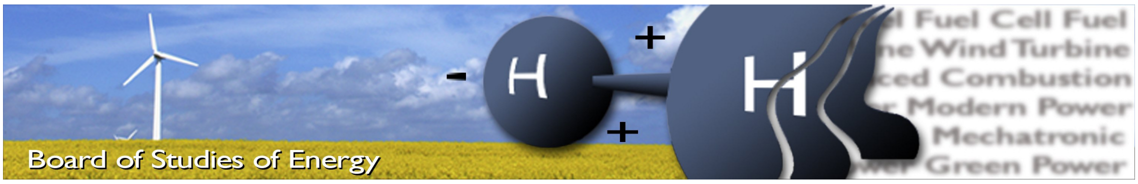

Title:	Experimental Investigation of a small width Heat-Sink with considerations for use with Thermo Electric Generators
Semester:	4th, Thermal Energy and Process Engineering
Semester theme:	Masters thesis
Project period:	01.02.2011 - 31.05.2011
ECTS:	30
Supervisor:	Lasse Rosendahl & Henrik Sørensen

ABSTRACT:

This masters thesis investigates the phenomena related to microchannels and discuses how these can be used with Thermo Electric Generators. State of the art of the system level TEG is discussed and a number of methods for choosing the optimal heat sink design is discussed. An experiment is performed on a mini channel to investigate the flow phenomena's related to the small dimensions. This is done in two ways, first an integral approach where UA values are determined and existing correlations compared to the measured average Nusselt number. And again with a novel experimental design involving Particle Image Velocimitry and Planar Laser Induced Fluorescence. This way it is tried to determine the local Nusselt values with direct and non-intrusive measuring methods. It is concluded that it is possible to resolve both the thermal and hydrodynamical boundary layers but not to a degree of precision that allows determination of the Nusselt number. A number of suggestions are made for further improvements.

Lars KUUR

Copies:	4
Pages, total:	XX
Appendix:	XX
Supplements:	None

By signing this document, each member of the group confirms that all participated in the project work and thereby all members are collectively liable for the content of the report.

Introduction

Microchannels, which is a common name for channels with dimensions in μ scale, is interesting both in industry perspectives and in the research communities. Originally conceived as a method of handling the increasing requirements for heat removal from electronics devices, it has now diffused into many other areas where the small sizes, high heat transfer coefficient and simple working mechanism are superior to other methods. The motivation for microchannels is that as the diameters of the channels are reduced the heat transfer increases. This increase happens at the cost of higher pressure loss, but until a certain point, dependent on design conditions, it is more advantageous to accept the pressure loss compared with using a bigger heat sink. The applications that microchannels are being envisioned for are tremendous and microchannels can potentially replace many existing heat-exchanger solutions. One such application is a Thermo Electric Generators (TEG), they are devices that converts heat energy to electrical power. With a temperature gradient the Peltier-Seebeck effect will occur and from this energy can be extracted. TEG's is a field where recent developments have increased the need for better thermal management.

A microchannel is a channel in a heat sink that has width, height or diameter between $1000\mu m$ and $1\mu m$. Or that is at-least the most strict definition. Many designs have been presented in the literature, for inspiration a few are shown in figure 0.1

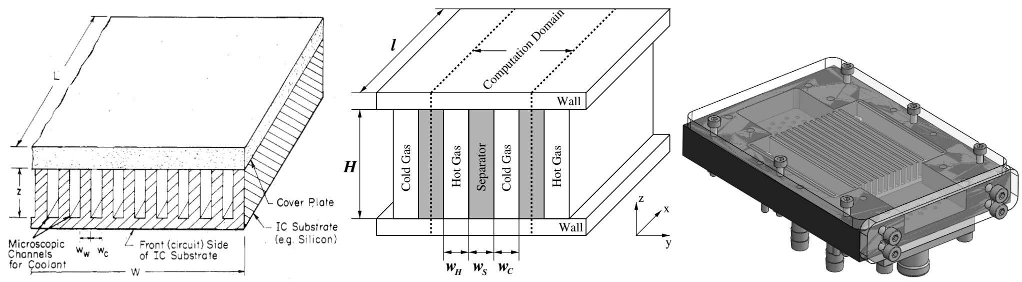

(a) *The original setup proposed by Tuckerman and Pease (1981)* **(b)** *Parallel gas heat exchanger from (Foli et al., 2006)* **(c)** *The setup used in this thesis*

Figure 0.1: *Two setup from literature and the one used in this thesis.*

The ability to predict the performance relies on the ability to predict flow phenomena's inside the channel with the applied boundary conditions. As a designer it is important to have tools such as correlations available to both make initial designs but also to validate results and numerical investigations. A good design will then be one with the best compromise between pressure loss, heat transfer coefficient and numerous other parameters such as, but not exhaustive, size and weight and price. It would be interesting to investigate how modern measurement equipment can be combined with known literature in consideration of the final application.

Project Scope Description and Problem Statement

The purpose of this project is to take the first steps towards a complete analysis for designing a microchannel for a TEG's thermal management system. Ideally it should be possible to follow these steps and design for most applications. These first steps means that a number of topics are covered in depth. A setup for an integral experimental approach, a setup for flow phenomena investigation and a review of current state of the art for microchannel design and TEG's on a system basis are presented. The concept being, that future works can apply the theory and find a design and experimentally investigate this.

A gap is seen in the present literature concerning advanced experimental investigations of the developing zones in small scale heat sinks. Special attention are given to this subject. The literature does provide a good description for the ideal cases, the gap is seen for more practical cases, such as heat exchangers with isolated top plates and non-ideal fins. Being able to experimentally determine the velocity and thermal map is especially of importance these years, considering the wide use of CFD.

A problem statement can then be formulated as:

What is the current state of the art for design of microchannels using analytical approaches and how can this be validated and improved with classic and advanced experimental methods?

To answer this three papers are presented.

Organization of the Thesis

The main body of this masters thesis consists of three papers. Each paper deals with a subject in a closed form and can be read independently of one another. With the combined knowledge of all three papers it should be possible to provide and answer to the problem statement.

The first paper named *Thermal management of a TEG using an optimisation scheme for microchannels* presents a discussion of state of the art in a generalised term for TEG's. Mostly the focus for that part is on the economics and discussions of initiatives started by the various actors. That is followed by a review of a classic microchannel optimisation scheme followed by a short review of the state of the art. The reason for writting this paper, is to provide a background information and putting the work into a context.

The second paper is entitled *Experimental Investigation of a Heat-Sink*. It concerns an integral approach that has been used to study the heat sink. To do this a design for a test rig is proposed. It is shown that the experimental setup in it's simple configuration can determine characteristic numbers such as Nusselt that fits well with similar numbers from literature. Some effort are put into showing the uncertainties with this experiment and reflections of the results are made. This paper is important because the more advanced methods are founded on the design presented herein. In perspective to other works this paper does not contribute anything new but more shows that the experiment setup is valid.

In the paper *Investigation of hydro-dynamically and thermally developing flow distribution with optical measurements on a small width heat sink* a novel method for investigation of a heat sink is presented. A thorough discussion of the governing equations and reflections are made on how to best find especially the Nusselt number using the two non-intrusive methods Particle Imaging velocimetry (PIV) and Planar Laser Induced Fluorescence (PLIF). The problem is approached with a discussion of some of the more important papers in this area followed by an analytical discussion. Based on these discussions two methods are proposed for using the PIV and PLIF information. One method utilizes the actual pixel-pr-pixel information captured by the PLIF system, and one does an energy balance on a discrete scheme. It is discussed that both methods could be improved if it could be combined with correlated PIV measurements. Data obtained for the PLIF calibration is presented and methods for how to do the calibration calculations with a novel Matlab^{TM} code is described. The experimental result is then presented and the two experimental methods compared. The results of PIV in the experiment is also treated and the finally the combination of PIV and PLIF. This paper serves to present the results of the advanced study that it was chosen to conduct. It uses the experimental setup described in the previous paper with slight modifications. Many of the methods and ideas presented are new to

the field. A consequence of this is a number of problems, but the paper shows the potential of the methods.
The entire thesis is finished with a conclusion and discussion.

Contents

Contents

Thermal management of a TEG using an optimisation scheme for microchannels

LARS KUUR
Department of Energy Technology
Aalborg University

lkuur07 @student.aau.dk

***Abstract*—A review of open literature describing TEG's with focus on applications and status of research. Perspectives for the TEG technology in a system perspective is discussed with some considerations of the economy and expected future developments. Finds that thermal management is becoming increasingly more important for a successful system. Based on this considers methods of using microchannel heat exchangers as a means of thermal management, with special attention to rectangular ducts. A scheme for systematic design of a micro channel heat exchanger for a TEG application are discussed.**

I. INTRODUCTION

THE continued demand for more energy efficient solutions pushes the demand for ways of recovering and transferring heat. Not only in conventional systems normally seen in the paradigm of thermal systems engineering, but also in systems with low thermal gradients, confined space and with limited thermal power available. One technology that operates in this evolving area is the Thermal Electric Generators (TEG's). Riffat and Ma (2003) conduct a review of potential applications and sets the following topics as critical for evaluating TEG for an application

- Running costs
- Module costs

Notice that there is no maintenance costs, this is because one of the main advantages of TEG's is long life expectancy and no moving parts. The thermoelectric generators driving the NASA Voyager probes now $17.7 \cdot 10^9$ km from earth is probably the best known example of this NASA (2011). The running costs is the fuel consumed for running the TEG. With commercially available 5% efficiency and with a future goal as high as 15% efficiency (Chen et al., 2010)(Riffat and Ma, 2003) it is still not near competing with other power generating systems. But the unique methods that the TEG can be integrated into a system allows it to be used in situations where alternative systems is expensive or impossible, where reliability and/or silence is valued highly. Often this will be in waste heat recovery. If there is no alternative to using the TEG, then the running cost is zero[1]. The module costs will still be relevant. (Riffat and Ma, 2003) finds commercial prices at $4^{£}/_{W}$. Very few papers dedicates them self to investigating or even discussing the economical prospects much further.

[1]Assuming no negative effects from having the module implemented

One very recent example of cost oriented research is (Ford Motor, 2011) which makes a rough estimate of the potential for TEG heat recovery in cars. Ford Motor (2011)finds savings between 0.2 and 0.4 $^{L}/_{100km}$ when the car is running a regulatory cycle, it is estimated to be higher in actual use. Although a bit tedious, it seems proper to make the basic calculations at this point in time, as in equation 1.

$$\overbrace{B(m)_{unit}}^{\textit{Balance}} = \overbrace{-(B_{\textit{TEG cost pr watt}} + B_{\textit{TEG cost pr watt}} \cdot ((1+r)^m - 1))}^{\textit{One time expense and compound interest}} + \underbrace{m \cdot B_{\textit{Energy cost pr Joule}} \cdot ((1+r)^m - 1)}_{\textit{Cost for energy over m time}} \tag{1}$$

Where $B(m)_{unit}$ is the balance at time m for one unit (1 Watt TEG energy installed). $B_{\textit{TEG cost pr watt}}$ is a one time expenses for installation of the system. $B_{\textit{Energy cost pr Joule}}$ is the end cost for one unit of energy which should have been supplied if the TEG havent, it is calculated as equation 2

$$B_{\textit{Energy cost pr Joule}} = \frac{B_{\textit{Input energy cost pr Joule}}}{\eta_{\textit{conv eff}}} \tag{2}$$

As an example it is interesting to find how long time (m) a car must run so that the saved gas costs exceeds the costs for the module. For reference, at an 4% interest rate, gas price at 1£, gas energy density of 34.8 $^{MJ}/_{L}$ and 20% energy conversion rate from chemical to electric it will take 4.9 years of the engine running. A gas price of 1£ may be low, but the nature of the equations, makes it so that when doubling the gas price to $2^{£}/_{L}$ it will still take 3.4 years of non-stop driving.

Ideally to find the system saving for a given installed system one needs to multiply the power installed, as in equation 3

$$B(m)_{sys} = B(m)_{unit} \cdot P_{installed} \qquad P_{installed} \leq P_{max} \tag{3}$$

Where P_{max} is the limit for how much can actually be installed in the system. Again for cars, (Stabler, 2011) considers the upper potential for the fuel economy savings. They find that just replacing the alternator is at most 1 to 4% saving, but also considers other applications such as faster engine warm up and electrically driving secondary engine systems such as coolant pumps, this is 0.5-5%. But Stabler (2011) also finds that the system will have negative effects, the increased weight of the system will have a negative impact between -0.5 to -1% [2]. This is an example of how a TEG system may not scale linearly as supposed in equation 3. Replacing the alternator is more beneficial then replacing a mechanical pump. For the system integration a number of considerations must also be made. The TEG must be regulated to give out the desired voltage, the weight and cost when scaling of such systems are still being investigated.

Focusing on the cost per. Watt overall two approaches for development exists:

- Develop low cost TEG systems
- Develop TEG systems with a higher efficiency

One promising method of cost reduction is with printed thin film TEG's (Xiao et al., 2008) and (Lee et al., 2011). (Xiao et al., 2008) reviews much of the ongoing research, but also focuses on the potential for high efficiency film, Xiao et al. (2008) remarks that although significant progress is being made the research happening is now still at a stage where the reported properties are difficult to compare. Lee et al. (2011) focuses on ZnSb film (ZinkAntimony). This is to eliminate tellurium (Te) as it is both toxic, a rare material and expensive. Lee et al. (2011) argues that not only should the production process be cost optimized, the materials used must also come cheap. Lee et al. (2011) successfully demonstrates a fin film with ZnSb[3].

On the subject of improving the efficiency numerous approaches within the material science exists. (Vining, 2009),(Vining, 2007) presents a commentary on the development. A considerable increase in efficiency is documented in the later years, but many results are obtained under laboratory conditions and are unstable.

In figure 1 a comparison is shown to illustrate the potential. Vining (2009) mentions that the equations may tend to over-predict the achieved efficiency, but it serves as a good indication. ZT is called the figure of merit and it is a means typically used to characterise the performance of a material for thermoelectric devices.

For figure 1 to have most meaning it seems important to present the graph shown in figure 2 as well. It was presented by Vining (2007) who in turn adopted (and updated) it from Dubois (1999).

But the main problem remains, as pointed out by Vining (2009), that although the development have shown very promising results the last years, the efficiency numbers that are now considered realistic in a foreseeable future, is still less efficient then low-end established methods. Also Vining (2009) criticizes the paradigm that researchers always compare the TEG waste heat recovery systems to status qua. (Vining, 2009) remarks that two of the major car brands have developed mechanical waste heat recovery systems that gives higher fuel savings then what is estimated to be gained with the 20% conversion efficiency that US Department Of Energy (DOE) considers a significant future milestone for on-board TEG's DoE (2009).

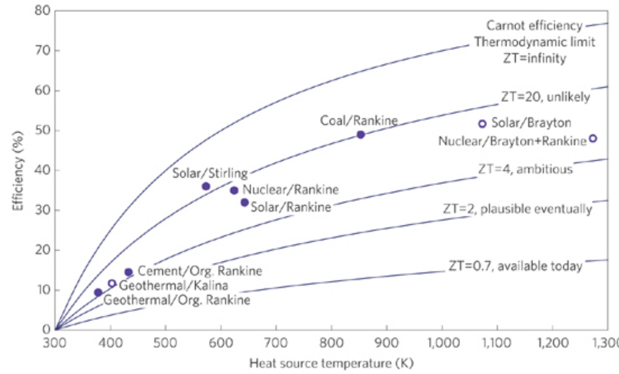

Figure 1. Comparison of thermoelectric generators against established methods and with changing temperature differences. From Vining (2009)

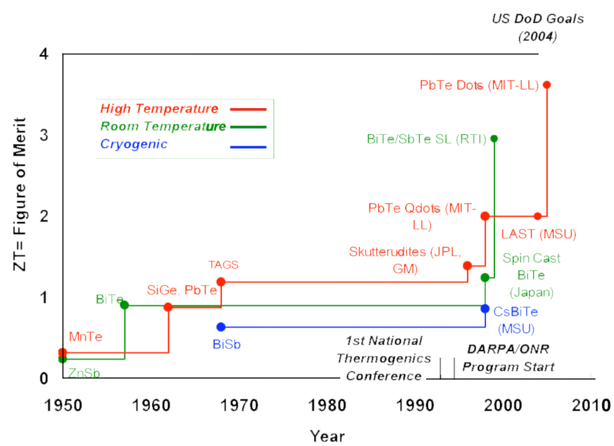

Figure 2. In the last years the development within thermoelectric materials have been significant. Modified from Vining (2007) who adopted and updated it from Dubois (1999).

Despite of this, if the TEG does not prevail in all areas the expected areas of use currently being discussed (Riffat and Ma, 2003) will still open a significant market.

Most of the documents mentioned at this point focuses on the material properties. As has been shown it retards the potential significantly. But it has also been shown that much of the recent research has moved the technology. This has called for system level approaches. NSF (2010) defined the areas requiring more research by the ways of figure 3.

Although the figure 3 is made for the vehicle applications it can be broadly applied.

1) Materials: The materials used, cost, efficiency and availability
2) Thermal management: Obtaining the best possible temperature distribution. Both the behaviour of the distributions in various operating modes. Ensuring heating and cooling. But also obtaining this with as few penalties as

[2]Another subject little discussed is the increased exhaust back pressure which reduces engine effect

[3]It is remarked that not all TEG's are with Te, but it is significantly represented in current and proposed designs

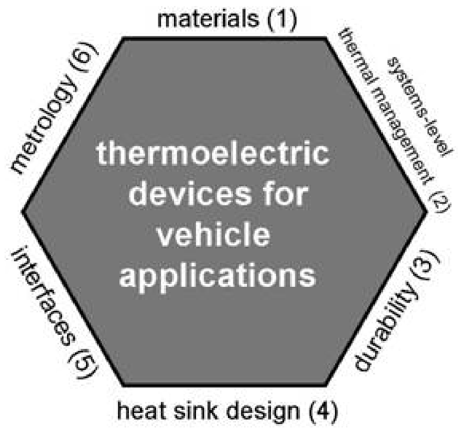

Figure 3. DoE and NSF called for applicants for a grant in 2010, they defined the system requiring further research as this figure NSF (2010).

possible (costs, pumping power, weight).

3) Durability: Ensuring a life expectancy that matches the parent system (for cars DoE says 15 years)
4) Interfaces: The nature of the possible applications where TEG's are relevant - Places where other technology doesnt work - means that the system experiences conditions such as high temperature swings and it must not de-laminate. Also the technology it self has a significant number of interfaces that must not fail thermally or electrically.
5) Heat sink design: The heat sink must have low thermal resistance that allows it to loose it's heat to the surroundings. At as little power costs as possible.
6) Methodology: As has been discussed in this paper, much of the current research is hard to compare due to lag of established scientific and industrial standards. Methods of comparing the entire TEG systems must be developed

As a summary, it seems that the first move from niche to broad market will be in the car industry. However more areas will follow it seems. One not so obvious advantage with TEG's, is that they do not suffer from many technology barriers when changing application. Assuming that the thermal aspects can be handled the know-how from using TEG's in cars can readily be moved to applications with large scale Combined Heat and Power (CHP) plants as Chen et al. (2010) suggests or to low-tech wood stoves in developing countries as suggested by Champier et al. (2011) .

But this wide possible expected use requires careful considerations in how the correct thermal management should be chosen to best suit an given application.

II. Thermal management using micro-channels

Many works have been published regarding thermal management with micro-channels. Tuckerman and Pease (1981) is widely regarded as the first significant paper about micro channels. Tuckerman and Pease (1981) made a experimental setup where they achieved very small thermal resistance. The reasoning is simple. Consider that the Nusselt number can be considered dependent of the diameter[4] and x as in equation 6.

$$Nu \propto \left(\frac{x}{D_h Re Pr}\right)^{-1/3} \tag{4}$$

Equation 6 exists in many varieties with many different constants fitted. But see that it is monotonically decreasing by x. It can be considered constant as $x/(D_h Re Pr) \geq 0.02$ is satisfied. Then the convective heat transfer coefficient h can be found as equation 5

$$h = \frac{k_f Nu}{D_h} \tag{5}$$

Taking a close look at the Nusselt number, with Reynolds number written out:

$$Nu \propto \left(\frac{x}{D_h \frac{D_h \dot{V} D_h^{-2} \rho}{\mu} Pr}\right)^{-1/3} \tag{6}$$

$$\rightarrow Nu \propto \left(\frac{x}{\frac{\dot{V}\rho}{\mu} Pr}\right)^{-1/3} \tag{7}$$

Nusselt number is then independent of D_h. h will then be reciprocal as a function of D_h. The smaller D_h, the higher the convective heat transfer constant h. Although simple it differs from common practice, heat exchangers was (are) typically designed so to get the highest effective surface areas.

In the following derivations we find the equations described originally by Tuckerman and Pease (1981). Most of the equations are simplifications and makes assumption. It will later be described how this approach can be expanded to overcome the restrictions in the method.

Heat transfer can be considered with an analogy to electric circuits. Considering a heat exchanger with an outlet / inlet as shown in figure 4. Assuming that the surface T_{const} is experiencing some thermal boundary condition, for example constant temperature.

A heat transfer optimization problem can then be described as equation 8.

$$R = \overbrace{R_{cond}}^{L/k_w A_s} + \overbrace{R_{conv}}^{1/h A_s} + \overbrace{R_{heat}}^{1/\dot{m} c_p} \tag{8}$$

It should be recognised that the first two terms (R_{cond} & R_{conv}) resemble the well known terms from the resistance heat transfer analogy. The last expression (R_{heat}) is the heat transferred to the fluid as if: $Q = \frac{1}{R_{heat}} \Delta T$. Considering the obvious interrelation it should be recognised how minimising all resistances in this way will give the highest heat transfer.

Although repetition we will now derive the expressions used by Tuckerman and Pease (1981) based on analysis approaches

[4]Be it hydraulic or actual round channels

used by White (2006). Later papers on the subject all uses the same methodology although with more advanced governing equations, boundary conditions and more free variables. The schematic of the fin is shown in figure 4.

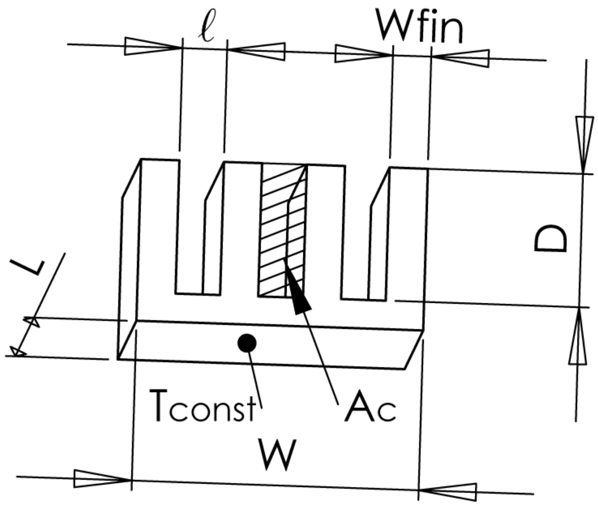

Figure 4. Schematic of the heat sink.

R_{cond} is neglected in most practical situations, this is because it can be neglected in comparison to the two other terms.

Looking at the thermal resistance, R_{heat}, it can be rewritten for the explicit flow velocity, as eqn. 9.

$$R_{heat} = \frac{1}{\rho c_p \dot{V}} = \frac{1}{\rho c_p U_m D \ell} \tag{9}$$

It could be interesting to involve U_m in a form that has more physical meaning. As shown in equation 10

$$f = \frac{\tau_w}{\frac{1}{2}\rho U_m^2} \tag{10}$$

Where the fanning friction factor (f), friction factor from this point, requires that the wall shear stress (τ_w) is known White (2006). It can be defined as:

$$\tau_w = \mu \frac{\partial U}{\partial y} \tag{11}$$

Where y is the distance from wall towards the centre and with the assumption of flow parallel to the wall. Obviously 11 is not very useful for finding an actual solution.

Continuous effort are put into finding correlations for the friction factor under special conditions, such as complicated boundary conditions, simultaneous thermal and hydrodynamically developing flows, and probably where the most effort are being spent at this period in time, with the advances in computational power, research in transient flows.

For Tuckerman and Pease (1981) the approach is less complicated. Considering just two plates parallel to one another. Then the flow condition can be reduced to Poiseulille flow.

Where it can be said that:

$$U = U_{max}\left(1 - \frac{y^2}{\ell^2}\right) \tag{12}$$

$$\dot{V}_{unit} = \int_{-\ell}^{\ell} U dy = \frac{4\ell U_{max} n}{3} \tag{13}$$

$$U_{mean} = \frac{\dot{V}_{unit}}{2\ell} = \frac{2}{3} U_{max} n \tag{14}$$

Then we can rewrite 14 to get U_{max} explicit. It then becomes: $U_{max} = U_{mean}3/2$. Then to find τ_w:

$$\tau_w = \mu \frac{dU}{d\ell} = \frac{2U_{max}\mu y^2}{\ell^3} = \frac{3U_{mean}\mu y^2}{D^3 n} \tag{15}$$

$$\rightarrow \tau_w = \left.\frac{3U_{mean}\mu}{Dn}\right|_{y=D} \tag{16}$$

We can then find the friction factor:

$$f = \frac{\tau_w}{\frac{1}{2}\rho U_{mean}^2} = \frac{6\mu}{\ell U_{mean}\rho n} \tag{17}$$

Another expression exists however, considering that the friction factor is related to the pressure loss, for laminar flow between two plates this can be written as:

$$f = \frac{\Delta p \ell}{2U_{mean}^2 L \rho} \tag{18}$$

Putting 17 equal to 18 and solving for the U_{mean} then yields:

$$U_{mean} = \frac{\ell^2 \Delta p n}{12 L \mu} \tag{19}$$

Now returning to 9, we replace U_{mean} with 19 and find that:

$$R_{heat} = \frac{1}{\rho c_p U_m D \ell} = \frac{12 L \mu}{c_p \ell^3 D \Delta p \rho n} \tag{20}$$

Now it should be possible to see that an optimisation will need to deal with both channel width and height. Equation 20 does not describe anything about the wall width, that is unfortunate as it is beneficial to have this as an variable. The thinner walls, the more channels are possible across the total width W.

This could be solved by just ignoring it for the R_{heat} but Tuckerman and Pease (1981) presents a more elegant solution, by setting α as an surface area multiplication factor. In continuum of the assumption that the top and bottom can be ignored, it is defined as:

$$\alpha = \frac{2D}{\ell + W_{fin}} \tag{21}$$

With the declaration of α and using[5] W we can now rewrite 20 and find the expression for R_{heat} that was actually used by Tuckerman and Pease (1981), as shown in equation 22

$$R_{heat} = \frac{24L\mu}{c_p\ell^3\Delta p\rho\alpha} \tag{22}$$

The most severe limitations for Tuckerman and Pease (1981) derivation is the assumption of parallel plates and fully developed (Poiseulille) flow.

To continue the analytical approach we consider R_{conv}. Recall that from 8 we saw the definition. With the use of α and η[6] and Nusselt number[7] and hydraulic diameter[8] we can describe the effective convective resistance as:

$$R_{conv} = \frac{1}{hA_s} = \frac{2\ell}{k_f Nu\alpha LW\eta} \tag{23}$$

Where we will need to describe the fin efficiency in more detail. Analytical expressions do exists, however with the assumption of:

- one dimensional conduction
- constant material properties
- constant heat transfer coefficient
- no radiation
- uniform fin base temperature
- $\star$: $L \gg W_{fin}\ell$ (Used to simplify equation 27)

Then summarising[9] the argumentation from Incropera et al. (2007):

Uniform rectangular fins with insulated tips can be shown to have a heat transfer as:

$$\dot{q}_{fin} = \sqrt{hP_{fin}k_{fin}A_{c,fin}}\ \ tanh(mD)(T_{base} - T_{fluid}) \tag{24}$$

Where m is a grouping of a part of the derived result.

And the heat transfer for an similar fin but with infinite conductivity:

$$\dot{q}_{fin} = hP_{fin}D(T_{base} - T_{fluid}) \tag{25}$$

Then taking the ratio between 24 and 25 we get:

$$\eta = \frac{tanh(mD)}{mD} \tag{26}$$

Where m will be:

$$m = \sqrt{\frac{hP_{fin}}{k_{fin}A_{c,fin}}} \overset{\star}{\approx} \sqrt{\frac{2h}{k_{fin}\ell W_{fin}}} \tag{27}$$

At this point the system of equations are described. Now it is a matter of solving the problem. It can be seen that R_{conv} is proportional to ℓ, and that R_{heat} is reciprocal as ℓ^{-3}. An optimum solution do exist and the reason why R_{heat} is included should be clear.

The remaining of Tuckerman and Pease (1981) will not be elaborated as the method is extensive in algebraic work[10] but not very interesting. Tuckerman and Pease (1981) choose to fix the design variables so that $W_{fin} \equiv \ell$ and $\alpha = \sqrt{k_w/k_f Nu}$ and $\Delta p = const$ that leaves just ℓ which can then be solved from the derivative of R. The final result is: $\ell = 2.29\sqrt[4]{\mu k_f L^2 Nu/\rho c_p \Delta p}$.

In short, the method for optimization of channels layout, is to describe the entire heat transfer problem in a way that allows the geometric variables and the power input to be design variables.

III. More extensive equations

As was mentioned, significant work has been put into describing the flow phenomenas in rectangular channels. The paper by Tuckerman and Pease (1981) was interesting in the sense that it described an systematic approach to utilising the developments in manufacturing technology for a new way of thinking heat exchangers, but the optimisation it self was retarded by the fixed variables and simplifications. Knight et al. (1992) is by many regarded as the next big landmark, Knight et al. (1992) tried with a more broad scheme that included re-writing for dimensionless variables, allowing a value for N_{work} (pumping work) to be set as an constraint. Also the scheme proposed included the equations for turbulent flow. The scheme now included bottom, no longer assuming two plates flow, and finally the width of the fin was included as an design variable in the Γ constant[11]. The improvements in the designs proposed by Tuckerman and Pease (1981) was as high as 22%. In figure 5 from Knight et al. (1992) it can be seen how allowing especially in the laminar regime the relaxation of the $\Gamma = 1$ gives significant improvements. This paper does not consider turbulent flows, but for reference it can also be seen how it behaves compared to the laminar solution, the reduction in thermal resistance comes at the cost of more pumping power required.

The suggested improvements still suffer from some major limitations, especially in the laminar regime.

- Does not consider developing flow in the laminar regime
- Depth of the channel fixed
- Outer dimensions (W,L) fixed
- Nusselt calculation assumes constant heat flux heating on all 4 sides of the channel.

[5] Defined as $W = n \cdot (\ell + W_{fin})$

[6] Fin efficiency

[7] $Nu = \frac{hD_h}{k_f} \rightarrow h = \frac{k_f Nu}{D_h}$

[8] We continue with the approximation that this can be considered as a two plate flow; then ($D_h = 2\ell$)

[9] We choose not to repeat the more basic derivations as the assumptions are less controversial

[10] At least with the level of detail used in this document

[11] $\Gamma = \frac{W_{fin}}{\ell}$

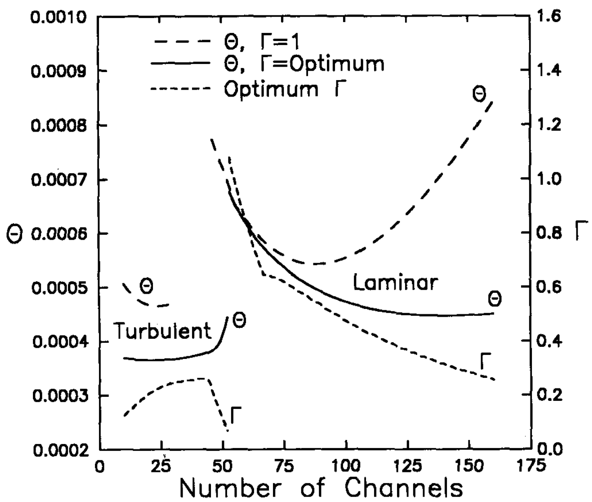

Figure 5. A comparison between the optimisation result from Tuckerman and Pease (1981)compared to Knight et al. (1992). From Knight et al. (1992)

In more recent years few works have been dedicated to the optimisation of microchannels. Foli et al. (2006) can probably be regarded as the current state of the art. First with a discussion where an analytical approach is used to optimise but CFD is used to get the actual results. That in contrast to the methods discussed above where the various properties such as Nusselt are also found analytical. This gives a graphical solution with pressure loss and heat flux as a function of aspect ratio. More significant is probably that Foli et al. (2006) manages to make a solution with a genetic optimisation algorithm (stochastic optimisation) that finds the optimum trade off between pressure drop and heat transfer. Since there is no cost coupling it gives a Pareto line. The algorithm automatically attempts various wall shapes and aspect ratios. The computational time is very extensive[12] and parts of the results can not be explained. But Foli et al. (2006) does show that this is a feasible method.

Few other has attempted new analytical schemes in recent years, this can probably be attributed to the fact that many of the basics for how to calculate Nusselt and friction and when transition occurs are still not settled. Morini (2004) presents an extensive review on most works. For laminar single phase flows Morini (2004) finds 8 works that concludes the Nusselt number increases with the Reynolds number, 7 works that finds it reduces and a few that are inconclusive. In the fully developed case the Nusselt number should be constant (White, 2006). Lee et al. (2005) presents an experiment and discussion on the field. It is argued (and to some extend shown) that many of the results being published as unique features for microchannels are more likely because of the fact that test microchannels are often short and therefore in the undeveloped regime. However many authors uses fully developed correlations. Also geometries and surface roughness may variate more than what some expects.

[12]Final result is 1 month computational time

With recent advances in measurements technique it has become possible to investigate the transition regime with μPIV. Among others Li et al. (2005) ,Li and Olsen (2006) and Sharp and Adrian (2004) compared the flow with macro scale, the first two found minor disagreement and the last found good agreement.

IV. Conclusion

It has been discussed how TEG's are being considered for use in fields where they despite poor efficiency can compete with other technologies. It has been shown how the economy aspects can be approached and the efficiency has been discussed. The main issue is that either the cost is too high or the efficiency is too low. But with increased efficiency better thermal management is required. On that context, microchannel schemes from literature on how to dimension has been discussed. It has been shown how the methods all to some extend has shortcomings. Especially in the developing regions, this is especially worrying as the TEG's will require as high a temperature difference as possible and a small number of units. A TEG may then have a heat exhchanger mounted that is short in this way. More research should be put into understanding the inlet thermal and hydrodynamic boundary layers at small channel sizes.

References

Champier, D., J. Bedecarrats, T. Kousksou, M. Rivaletto, F. Strub, and P. Pignolet (2011). Study of a TE (thermoelectric) generator incorporated in a multifunction wood stove. *Energy*.

Chen, M., H. Lund, L. A. Rosendahl, and T. J. Condra (2010). Energy efficiency analysis and impact evaluation of the application of thermoelectric power cycle to today's chp systems. *Applied Energy 87*(4), 1231 – 1238.

DoE (2009). Deep-dive. Technical report.

Dubois, L. (1999). An introduction to the DARPA program in advanced thermoelectric materials and devices. In *Thermoelectrics, 1999. Eighteenth International Conference on*, pp. 1–4. IEEE.

Foli, K., T. Okabe, M. Olhofer, Y. Jin, and B. Sendhoff (2006). Optimization of micro heat exchanger: Cfd, analytical approach and multi-objective evolutionary algorithms. *International Journal of Heat and Mass Transfer 49*(5-6), 1090–1099.

Ford Motor (2011, Jan). Doe phase 5 teg program. In *DoE Thermoelectric Applications Workshop*.

Incropera, F. P., D. P. DeWitt, T. L. Bergman, and A. S. Lavine (2007). *Fundamentals of heat and mass transfer.* Hoboken, NJ: John Wiley. ID: 62532755.

Knight, R., D. Hall, J. Goodling, and R. Jaeger (1992, October). Heat sink optimization with application to microchannels. *Components, Hybrids, and Manufacturing Technology, IEEE Transactions on 15*(5), 832 –842.

Lee, H. B., J. H. We, H. J. Yang, K. Kim, K. C. Choi, and B. J. Cho (2011). Thermoelectric properties of screen-printed

znsb film. *Thin Solid Films In Press, Corrected Proof*, –
.

Lee, P., S. Garimella, and D. Liu (2005). Investigation of heat transfer in rectangular microchannels. *International Journal of Heat and Mass Transfer 48*(9), 1688–1704.

Li, H., R. Ewoldt, and M. Olsen (2005). Turbulent and transitional velocity measurements in a rectangular microchannel using microscopic particle image velocimetry. *Experimental thermal and fluid science 29*(4), 435–446.

Li, H. and M. Olsen (2006). Micropiv measurements of turbulent flow in square microchannels with hydraulic diameters from 200 [mu] m to 640 [mu] m. *International journal of heat and fluid flow 27*(1), 123–134.

Morini, G. (2004). Single-phase convective heat transfer in microchannels: a review of experimental results. *International Journal of Thermal Sciences 43*(7), 631–651.

NASA (2011). Voyager set to enter interstellar space. Technical report.

NSF, D. (2010). NSF/DOE Partnership on Thermoelectric Devices for Vehicle Applications - 2010 Solicitation.

Riffat, S. B. and X. Ma (2003). Thermoelectrics: a review of present and potential applications. *Applied Thermal Engineering 23*(8), 913 – 935.

Sharp, K. and R. Adrian (2004). Transition from laminar to turbulent flow in liquid filled microtubes. *Experiments in fluids 36*(5), 741–747.

Stabler, F. (2011, Jan). Benefits of thermoelectric technology for the automobile. In *DoE Thermoelectric Applications Workshop*.

Tuckerman, D. and R. Pease (1981, May). High-performance heat sinking for vlsi. *Electron Device Letters, IEEE 2*(5), 126 – 129.

Vining, C. B. (2007). Zt 3.5: Fifteen years of progress and things to come. In *European Conference on Thermoelectrics*.

Vining, C. B. (2009). An inconvenient truth about thermoelectrics. *Nature materials 8*, 83–85.

White, F. M. (2006). *Viscous fluid flow : (by) frank M. White.* (3rd ed.). New York: Mcgraw-Hill. ID: 301720193.

Xiao, F., C. Hangarter, B. Yoo, Y. Rheem, K.-H. Lee, and N. V. Myung (2008). Recent progress in electrodeposition of thermoelectric thin films and nanostructures. *Electrochimica Acta 53*(28), 8103 – 8117.

Experimental study of a Heat-Sink

LARS KUUR
Department of Energy Technology
Aalborg University

lkuur07 @student.aau.dk

***Abstract*—This paper concerns the experimental setup and determination of key characteristics for a heat sink. The fluid medium is water on both cold and warm side. The cold (25-30 C°) fluid flows through a fin heat exchanger enclosed in a way that allows for PIV and PLIF measurements. The warm side (60-65 C°) is injected on a flat plate with a high flow to get a uniform temperature distribution. It is found that the temperature increases 2-6 K on the cold side and UA values are shown in relation to mass flow and logarithmic mean temperature difference (LMTD). The channel is 7 mm deep and has a width of 2.35 mm the wall is 1.25 mm. The total length is 57.5 mm and the flow is across 10 channels.**

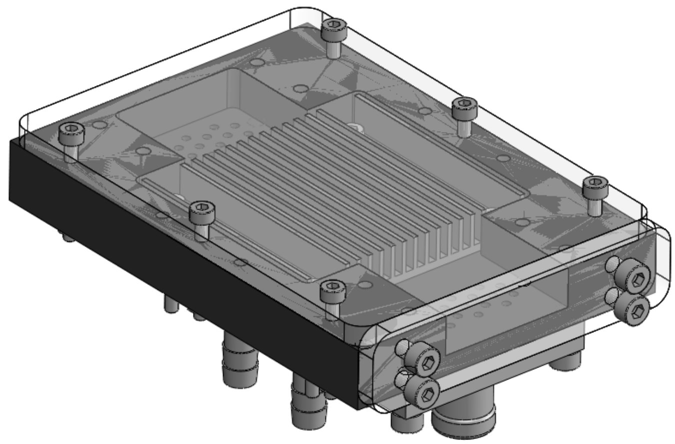

Figure 1. The body of the experiment, in centre the test section with the heat exchanger, to the right the acrylic transparent sheet for the laser sheet, inlet and outlet through a mesh to get a uniform flow field.

I. INTRODUCTION

THE aim of this paper is to present an experimental design that in a future work can be used to determine flow characteristics using Particle Image Velocimitry (PIV) and Planar Laser-Induced Fluorescence (PLIF). For more sophisticated methods such as PLIF and PIV, it is necessary that the experiment is well defined and it is desirable that an amount of reference properties are logged for in-situs validation and for later comparison with obtained results.

II. EXPERIMENTAL DESIGN

The experiment consists of an Polyoxymethylene (POM) block, this has a centre region where the heat exchanger is mounted. The inlet and outlet is designed so to get a well defined flow field into the test section. One side is left open so that an transparent acrylic sheet can be mounted[1]. The block is shown in figure 1.

On the backside, the hot side, is designed with an aluminium backplate and two inlet and two outlet fittings, the water is injected directly onto the heat exchanger backside. The backside configuration is shown in detail in figure 2

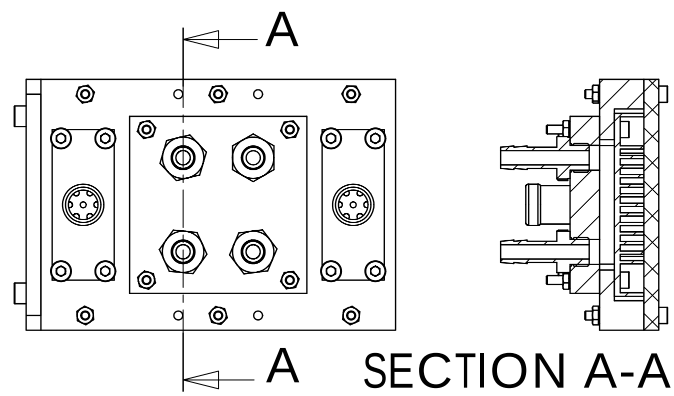

Figure 2. The setup seen from the back and a section cut. Hot inlet and outlet in the the four centre fittings. Cold in and outlet is the larger end fittings.

The cold water inlet and outlet is made in POM plastic with a manifold prior to the mesh in the main body. All seals are done using either silicone where disassembly is not later required and liquid gasket where it will be. The system is connected by a number of plastic tubes. The hot flow inlet is two small pumps joined into one which passes another pump and a flow sensor. The unusual pumping configuration

[1] For the laser sheet that will be applied later

is to achieve the desired flow with the pumps available [2]. The hot flow is taken and returned to a reservoir. This reservoir is a glass container placed on a lab combined heater and magnetic agitator. Temperature measurements on the hot flow is performed at the inlets and outlets and on the reservoir. The cold flow is cooled using a water to air active cooler on the inlet side. The reservoir itself is not cooled, but the thermal capacity is high because of the relative size. The flow is ensured with a pump and downstream a flow sensor is mounted. The cold side temperature measurements are performed in the manifolds prior to the meshed inlet. The setup with indications of where measurement are performed are shown in figure 3 and a photo from the laboratory displaying the actual configuration are seen in figure 4[3].

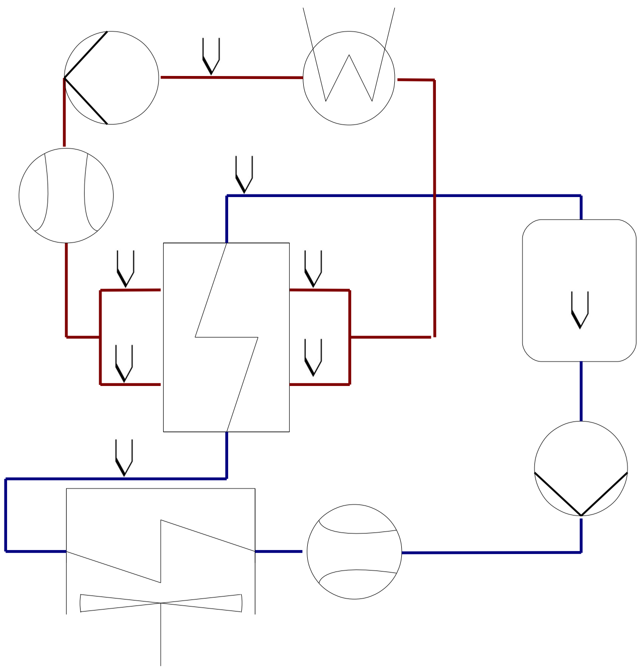

Figure 3. Schematic flow setup with thermocouples and flow sensors shown.

As can be seen from the picture in figure 4 the equipment for PIV and PLIF is included, it is however not active in the series of data treated in this document. When active the images will get a time code and basic informations to ensure correct synchronisation between the equipment.

The data loging is performed via National Instruments software LabView running on a desktop computer. The chassis is a NI cDAQ-9172 which connects via USB. It has the following modules mounted:

- NI 9213 16 channel Thermocouple module (for temperature measurements)
- NI 9401 8 channel Digital I/O module (for measuring pulse frequency from flowsensors)
- NI 9481 4 channel Electromechanical relay (for turning pumps and fan on/off)

[2]The pump configuration also allows for better fine tuning of the flow

[3]The flow sensor seen in the top right corner was replaced to improve accuracy

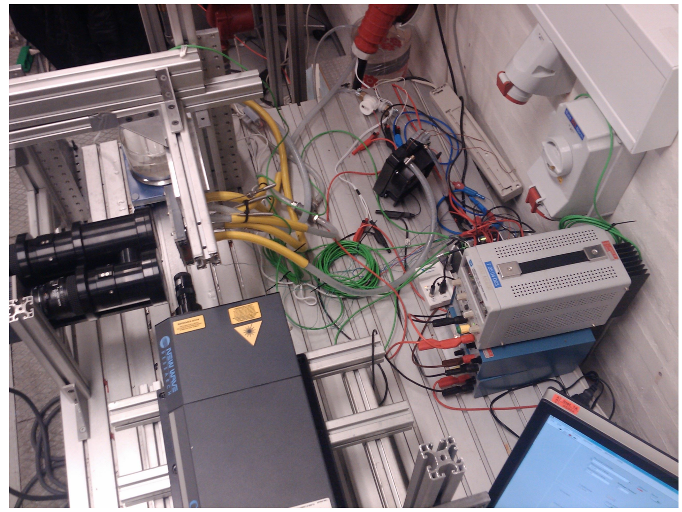

Figure 4. From left to right: Top corner, the heater and agitator; left centre, the splitter for the two cameras looking at the test section; lower left the dual laser. Center mid the tubes with thermocouples inserted into them. Right top the cold reservoir and the active cooler; lower right data logging equipment and three of the four power supplies; bottom right corner the monitor for control via LabView.

- NI 9263 4 channel Analog output (for use with PIV/PLIF)

The system is powered by one DC power supply for fan and the two hot and cold side pumping configurations. Making a total of 3 power supplies dedicated to this task. Flow is manually regulated with the DC voltage. For most cases the hot side pumps was kept constant at 12V and drawing 6-7A (72-84W) resulting in a flow of $\approx 4\ {}^{L}/_{min}$. To get the desired cold side flow the voltage typically ranged from 4-7V with $\approx$ 1-2A drawn. The pumps are general purpose with continuous flow and all rated for 12V. Fan was kept constant at max power. The flow-sensors are powered by a fourth power supply, the chosen sensors are shown in table II

Flow sensors

Name	Flow Range	Linearity at FSD	Frequency at FS
Cold flow			
RS 257-149	0.25-6.5 ${}^{L}/_{min}$	$\pm1\%$	500Hz
RS 511-3892 (2mm jet)	0.05-1.5 ${}^{L}/_{min}$	$\pm2\%$	175Hz
Hot flow			
Name	Flow Range	Linearity at FSD	Frequency at FS
RS 511-3892 (3mm jet)	0.15-4.5 ${}^{L}/_{min}$	$\pm1.5\%$	260Hz

Table I

FLOW SENSORS USED AND STATS AND UNCERTAINTIES. THE COLD FLOW SENSOR WAS CHANGED AFTER THE EXPERIMENT RESULTS TREATED IN THIS PAPER, BUT USED FOR THE PIV AND PLIF MEASUREMENTS AS IT HAS A BETTER SUITED FLOW SCALE

The error related to linearity and frequency will be calculated and shown when the results are discussed. The thermocouples are of the type K.

A. Experiment results

During the experiment the flow of the cold water and the logarithmic mean temperature difference was kept as variables. The hot flow was kept constant. The heat exchanger is then profiled as the UA values as a function of these two variables.

The results was gathered with several cycles, the temperature was reached for the hot water and a number of samples gathered, then a new cold flow was set and so it was repeated. In figure 5 and figure 6 the raw untreated results are shown for cold and hot side respectively.

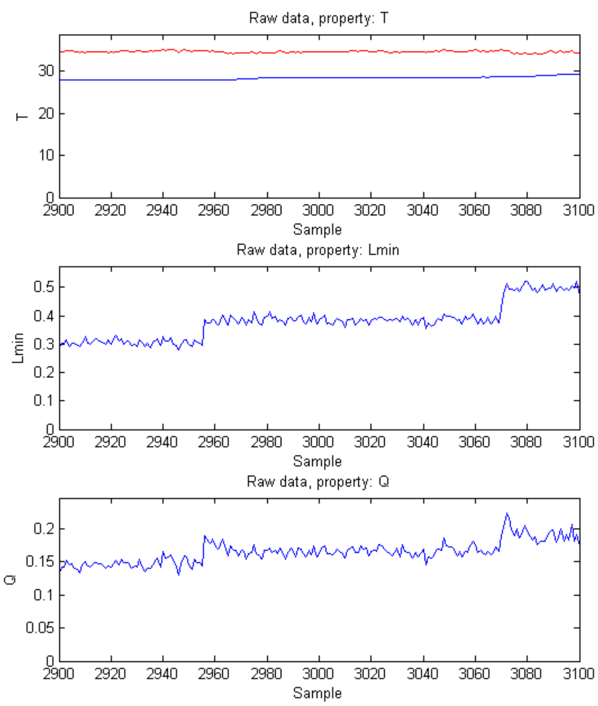

Figure 5. The untreated data for cold side.

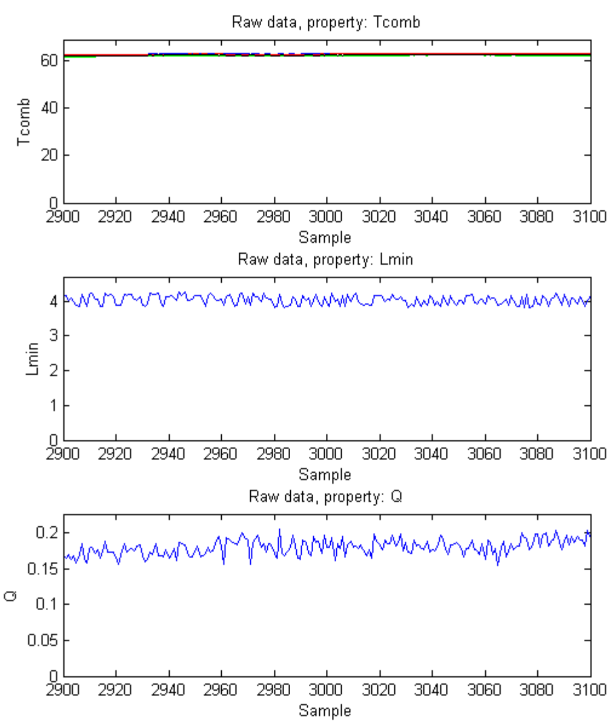

Figure 6. The untreated data for hot side.

A couple of things can immediately be seen, the cold flow out (red data series in upper left) is fluctuating a lot. These fluctuations are not seen when there is no thermal flux. It would seem that the fluctuations are related to a flow phenomena. Something that will be investigated further with the PLIF and PIV measurements. The fluctuations in the flow sensors measurements are obviously a major source of uncertainty. The fluctuations in the flow sensor measurements are overall the major contributor to the noise seen in the heat transfer (Q). It seems that part of the fluctuations is from the pulsation in the centrifugal pumps. Also the measurement was performed with the first flow sensor, giving slightly more scaling problems.

The worst outliers are later removed from the dataset, this is done with a 95% confidence interval for both temperature and mass flow. The data is segmented as can be seen, the applied conditions are assumed to be constant for each flow segment. These segments are taken as data-points.

The heat transferred (Q) is found with equation 1

$$Q = \dot{m} \cdot (h_{out} - h_{in}) \tag{1}$$

Where $\dot{m}$ is found using a temperature dependent viscosity. As was shown in figure 5 and 6 this is done for both cold and hot side. The LMTD value can be found as:

$$LMTD = \frac{\Delta T_a - \Delta T_b}{ln\left(\frac{\Delta T_a}{\Delta T_b}\right)} \tag{2}$$

Where $\Delta T_a = T_{hot} - T_{cold,in}$ and $\Delta T_a = T_{hot} - T_{cold,out}$ equation 2 is then reduced to 3.

$$LMTD = \frac{T_{cold,out} - T_{cold,in}}{ln\left(\frac{T_{hot}-T_{cold,in}}{T_{hot}-T_{cold,out}}\right)} \tag{3}$$

With this knowledge the UA value can be found as equation 4

$$\begin{aligned} Q &= UA \cdot LMTD \\ \rightarrow UA &= \frac{UA}{LMTD} \end{aligned} \tag{4}$$

It is then desired that:

$$\overline{UA}_i = f_{UA}(\overline{\dot{m}}_i, \overline{LMTD}_i) \tag{5}$$

Where i is the treated segment of data.

In figure 7 this is shown with the LMTD temperature shown as colour and mass flow on the x axis, notice that for both graphs the mass flow is the cold as the hot is kept constant.

The values for the right will be influenced by the lose of heat to the surroundings. This heat lose should be constant as the hot side temperature is close to constant for most data segments. This shows in the positive offset for all the data.

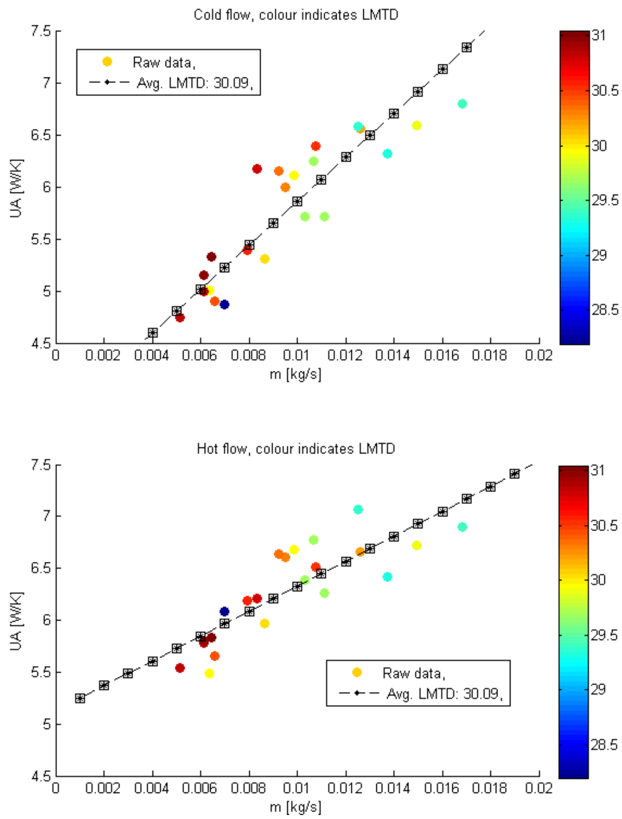

Figure 7. Using interpolation to generate points for a constant LMTD and varying mass flow.

Interpolation, in this case first order least squares method, can then be used to find a single line, so to express the UA value only as a function of cold mass flow. This is shown in figure 7.

Since the data is expected to behave linearly we can apply the linear interpolation with equation 6

$$UA_{p_0} = a_1\dot{m}(p_0) + a_2 \tag{6}$$

Where a is a constant coefficient. It is found as shown in equation 7 (Hooper, 2010)

$$\vec{a} = \frac{\begin{bmatrix} \dot{m}_{p_1} & 1 \\ & \ddots \\ \dot{m}_{p_n} & 1 \end{bmatrix}_{n\times 3}}{\begin{pmatrix} UA_{p_1} \\ \vdots \\ UA_{p_n} \end{pmatrix}} \tag{7}$$

The average LMTD value for all data points is 28.55 K. Looking at the line it can be seen that the offset difference between hot and cold side is about 0.8 at 0 flow. However the incline is not similar between hot and cold. This is because the hot side heat loss to the surroundings is unaffected by the increase in cold massflow. The hot side heat loss can be regarded as equation 8.

$$Q_{tot} = Q(\dot{m}_{cold}, LMTD)_{hot\rightarrow cold} + Q(0,0)_{surroundings} \tag{8}$$

.

Thus changing $\dot{m}_{cold}$ and *LMTD* has less effect for the hot side.

B. Treatment of uncertainties

The following significant contributors can be identified for figure 7

The uncertainties from fluctuations in the dataset is taken for every segment of data which gives a fixed mean. The linear interpolation is found by cross referencing, each known point is interpolated, the deviation from the known value to the predicted value is then used instead of a mean, as seen in equation 9

$$\frac{1}{n-1}\sum_{n=1}^{n}(\hat{UA}_{p_x} - UA_{p_x})^2 \tag{9}$$

Where $\hat{UA}_{p_x}$ is the predicted value.

For the thermocouples, it was seen that after having reached thermal equlibrium over night they assumed the same value with for any time a bigest diference between two thermocouples of 0.14 $°C$ and a mean 0.6, the errors was seen mostly as random and it was chosen not to set a comon zero. The difference between hot and cold side when assumed equlibrium was at most 0.5 $°C$, the effect on the temperature difference is found to be less then 1%. The thermocouples and system was not calibrated before use, a systematic error in the absolut reading may be present, however since it is foremost the differential values that are of interest this has little effect. Any such systematic error will only have an effect on the water property lookups, and the effect on this will be negligble. The aquisition system, the NI 9213 has a sensitivity of less than 0.02 $°C$.

For the experimental procedure some assumptions are made:

1) The cold flow is only affected by the heat-exchanger, no heat loss through the POM or acrylic sheet [4].
2) Even temperature across the entire back surface of the heat exchanger

For assumption one, the reservoir containing the cold water does heat over time. It was seen that at 5-6 K above room temperature the heat loss from the reservoir and the air to water heat exchanger gave a steady state condition. With a temperature increment of 6 degree from inlet to outlet the highest temperature difference from the surroundings to the fluid is then 12 K. This loss to the surroundings was investigated by stopping the hot flow pumps and letting the cold pump run [5]. The highest heat loss was found when the pump was running at the flow sensors maximum (1.5 $^{L}/_{min}$).

[4]Not the case for the hot flow as it is contained by a not isolated plate of aluminium

[5]The result of this was that the fluid was never heated, and the temperature difference was just 6 K and not the peak value 12 K

Name	Type	Property	$\bar{\sigma^2}$ cold flow	$\bar{\sigma^2}$ hot flow	$\frac{\sigma \cdot z}{\sqrt{n}}$ cold flow	$\frac{\sigma \cdot z}{\sqrt{n}}$ hot flow
		Uncertainties				
Linear interpolation	Precision	UA [W/K]	0.247	0.3314	0.1587	0.2020
Dataset	Fluctuations	UA [W/K]	0.222	0.3098	0.1505	0.1953
Sum	$\sqrt{X_1^2 + X_2^2 ...}$				0.2187	0.2810
		Errors				
Flow sensor	Non-linearity	Flow [L/min]	-	-	±0.0650	±0.0675
	Resolution	Flow	$min\,(f) = 24Hz$		$min\,(f) = 210Hz$	

Table II
CONTRIBUTORS TO UNCERTAINTIES AND ERRORS IN THE DATASET, Z=1.96 (0.95%).

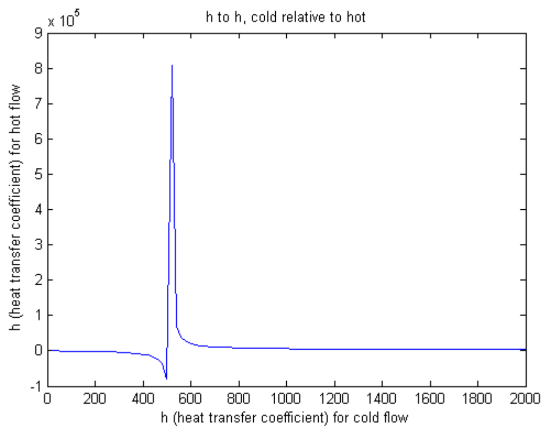

Figure 8. The heat transfer coefficient for the hot flow can not be neglected

At that point in time the biggest change in heat was 0.0136 W. When the system is active the heat transfer from hot to cold side is between 75-200 W. Despite the shortcomings of this small investigations, the loss is negligible. The assumption that there is no loss to the surroundings is reasonable.

In regards to assumption two; The hot-water inlet is chosen in a criss-cross pattern, so that when referring to figure 2 the upper left and lower right is hot water in, and the opposite are outlets. The biggest temperature drop, that is the highest inlet temperature versus lowest outlet ranges from 0.5 to 0.9 K the corresponding other inlet/outlet typically ranges from 0.25 to 0.6. When calculating the mean temperature difference the mean of all four are taken as the constant temperature for hot side. This introduces an absolute maximum temperature error of 0.45 K. It is also worth noticing that the choice of a criss-cross pattern means that flow from the upper left corner to the upper right corner is parallel while the lower right corner is counter current. This results in small variations in the temperature profile with a deviation from the mean of 0.15 K. More important is the heat transfer coefficient from water to the plate. Is it high enough to maintain almost the flow temperature on the plate.

This was investigated in figure 8

It can be seen that the function is discontinous, at the given conditions there is a lowest possible heat transfer coefficient for cold side at about 520 $W/(m^2K)$ Based on experience it is expected that the coefficient should be about 10 000. This is a worst case scenario However should it be that low, then the wall temperature will be 50 $°C$, such an error introduces up to 25 % uncertainties in the results. But it is difficult to say for certain if it is more or less. This experiment should be repeated with more sensors to get more information about this.

III. EVALUATION OF RESULTS

A number of expresions have been developed in literature, trying to predict the flow and thermal effects in small rectangular channels. Shah and London (1978) made a significant contribution to understanding heat transfer in more arbitrary geometries with different boundary conditions. Many attempts at predicting nusselt numbers are based on the assumption of fully developed flow, this is not the case in this experiment. The issue with the coupling of the thermal and hydrodynamic developing flow has been somewhat sucsesfull for flatplates White (2006), but semi empirical methods have been better for ducts flow. A more extensive review of the methods applied here, and an attempt at describing the flow phenomena can be found in Kuur (2011). Incropera et al. (2007) discusses the expected hydrodynamic and thermal entry length for circular pipes, by using the hydraulic diameter for a rectangular duct it is applied here, it is shown in equation 11.

$$L_h = 0.05Re \cdot d_h \tag{10}$$

$$L_{th} = 0.05Re \cdot Pr \cdot d_h \tag{11}$$

The lowest Reynold number is 128.46, this gives $min(L_h) = 0.0232m$ and $min(L_{th}) = 0.1283m$. The length of the channel is 0.0570 m. The highest Reynolds number is 430.377 which gives $L_h = 0.0777$. Qu and Mudawar (2002) finds that applying this method for rectangular channels may overestimate the length. The flow is expected to be thermally developing in the entire heatsink and the hydrodynamics may be considered either. In table III the equations used in this paper and selected properties are shown.

Finding the experimental Nu value can be done by equation 12.

$$Nu = \frac{h \cdot d_h}{k_f} \tag{12}$$

To find h we reconsider the UA expresion. First A can be found by finding the fin efficiency and then the efficient area of heat transfer. Fin efficiency is given as equation 14

Correlations applied

	Original geometry	Flow	Nu correlation
Peng and Peterson (1996)	Rectangular 3 heated sides	Developing Const Wall temp	$0.1165\left(\frac{d_h}{\ell+\ell\cdot\Gamma}\right)^{0.81}\gamma^{0.62}Pr^{1/3}$
Incropera et al. (2007) (Based on Hausen correlation)	Circular Circ. heating	Thermally developing Const Wall temp	$3.66+\frac{0.19(RePrD_h\cdot L^{-1})^{0.8}}{1+0.117(RePrd_h\cdot L^{-1})^{0.467}}$
Incropera et al. (2007) (Based on Sieder-Tate correlation)	Circular Circ. heating	Developing Const Wall temp Recommended range: $0.6 \leq Pr \geq 5$	$1.86\left(\frac{RePrD_h}{L}\right)^{1/3}\left(\frac{\mu}{\mu_s}\right)^{0.14}$
Lee and Garimella (2006) (Originates from Shah and London (1978).)	Rectangular 3 heated sides	Fully developed Const flux	$8.235(1-1.833\alpha^{-1}+3.767\alpha^{-2}-$ $-5.814\alpha^{-3}+5.361\alpha^{-4}-2\alpha^{-5})$
Kays et al. (2007) and Knight et al. (1992) (Originates from Shah and London (1978).) (Knight et al. (1992) uses a simpler fit version)	Rectangular 4 heated sides	Fully developed Const flux	$8.235(1-2.042\alpha^{-1}+3.085\alpha^{-2}-$ $2.477\alpha^{-3}+1.058\alpha^{-4}-0.186\alpha^{-5})$

Table III
CORRELATIONS USED TO PREDICT NU

$$m = \sqrt{\frac{hP_{fin}}{k_{fin}A_{c,fin}}} \approx \sqrt{\frac{2h}{k_{fin}\Gamma\ell}} \tag{13}$$

$$\eta = \frac{tanh(mD)}{mD} \tag{14}$$

Effective surface area is then given as equation 15

$$A_s = \frac{nWD}{n+\Gamma(n-1)} + 2\eta DL(n-1) \tag{15}$$

Then by using the known convective thermal resistance and comparing it to equation 17 Knight et al. (1992).

$$C1 = n + \Gamma(n-1) \tag{16}$$

$$\frac{k_f W}{hA_s} = \frac{2C1}{Nu^{L}/W(C1 + {}^{W}/D)(n + 2\eta^{D}/W(n-1)C1} \tag{17}$$

It is then a trivial to find η. It is almost constant at 0.836 or 83.6%. The surface area is found to be 82 cm^2. Already at this point experimental h (U) has been used. It should be consideres that it is composit in nature. It should be defined as:

$$UA_{avg} = \frac{1}{A_{\text{flat plate}}h_{\text{hot water}\rightarrow wall}} + \frac{L}{A_{wall}k_{wall}} + \frac{1}{A_{surf}h_{wall\rightarrow \text{cold water}}} \tag{18}$$

However, these are all considered minor and the interesting souce is with the h coefficient on cold side.

In figure 9 the result is shown.

It can be seen that those correlations only dependent on geometric properties does not change as a function of flow. This means that for some intervals they do a decent prediction. Lee, Perkins and Knight are all close with theyr fixed value. However it is most Peng's correlation that best captures the trens in the data. Even Lee et al. (2005) mentions that in the inlet area the correlation has shortcommings, this seems true considering that in the inlet the Nu value will be higher, so the correlation might underpredict the Nu value some. The acutal flow phenomena present here will be discussed further with the application of PIV and PLIF simultaniously.

IV. CONCLUSION

An experimental setup for charachterising a heat sink has been discused. It was found that it is possible to find both trends and usefull data in the obtained data. By expresion in the non-dimensional Nusselt number as a function of Reynolds and comparison between various correlations it has been shown that even though the correlations with some dependency of the massflow does predict the best result, the only geometry dependent correlations are able to predict a reasonable close Nusselft number. This is especially interesting for optimisation schemes as this decouples the calculation of Nusselt with first having determined the properties for the flow (h,Re,Pr etc). It is also seen that some methods are not very well suited to predict the values. Attempting to use Incropera et al. (2007) correlations developed for circular tubes for ducts did poorly, but it did capture the trens in the data, but with a significant overprediction of the values. A number of issues with the current experimental design has been found, these will be solved and a future work will investigate the channel flow PIV/PLIF, this will reveal more about the nature of the flow, to what extend is it thermally and fluiddynamically developing.

REFERENCES

Hooper, A. (2010). Multivariate data analysis course - tudelft, department of remote sensing. Technical report.

Incropera, F. P., D. P. DeWitt, T. L. Bergman, and A. S. Lavine (2007). *Fundamentals of heat and mass transfer.* Hoboken, NJ: John Wiley. ID: 62532755.

Kays, W. M., M. E. Crawford, and B. Weigand (2007). *Convective heat and mass transfer*. Boston [u.a.]: McGraw-Hill. ID: 699686337.

Knight, R., D. Hall, J. Goodling, and R. Jaeger (1992, October). Heat sink optimization with application to microchannels. *Components, Hybrids, and Manufacturing Technology, IEEE Transactions on 15*(5), 832 –842.

Kuur, L. (2011). Thermal management of a teg using an optimisation scheme for microchannels.

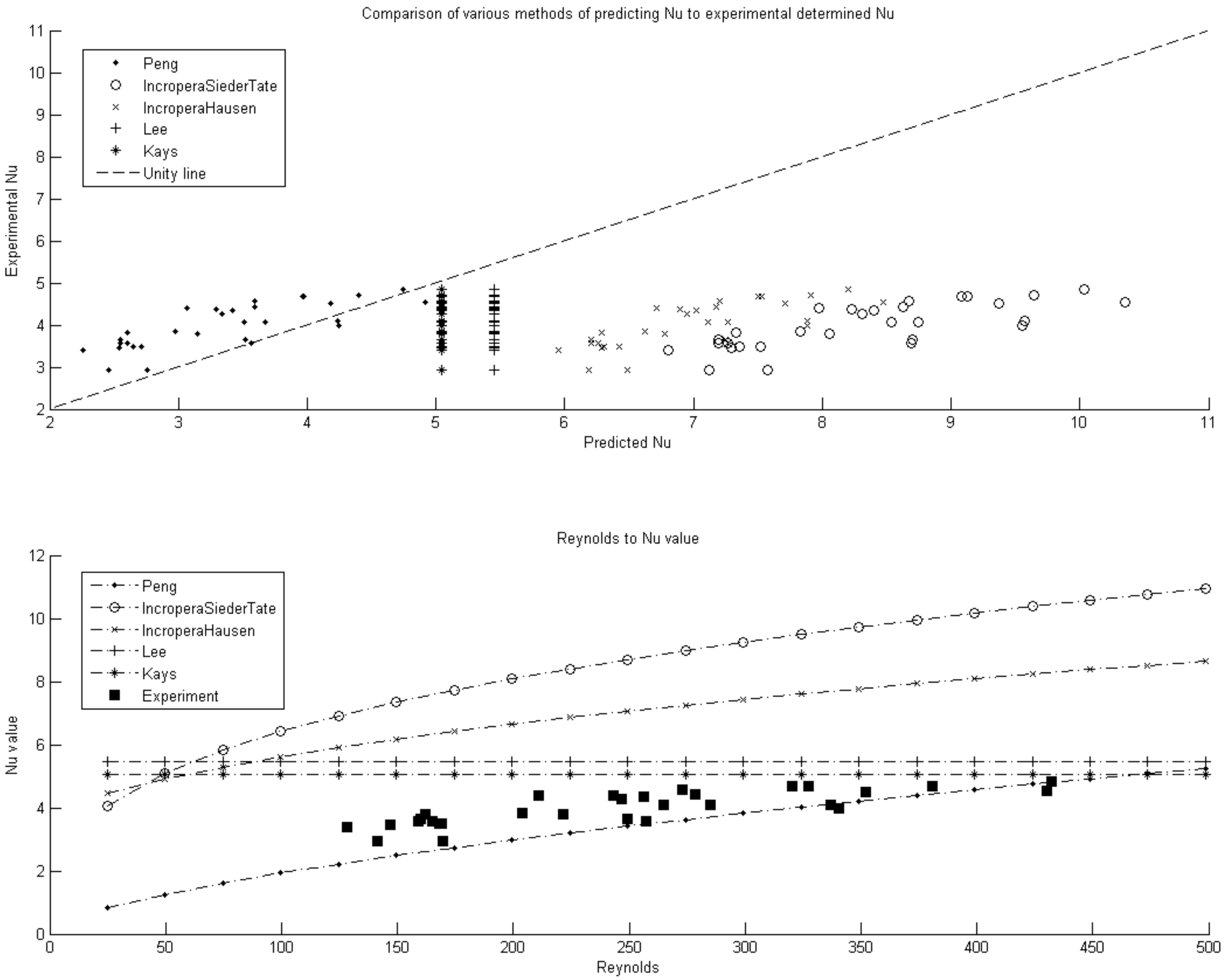

Figure 9. On top the comparison between predicted and actual Nu values, the close to unity the better agreement. On lower the Nu as function of Reynolds

Lee, P. and S. Garimella (2006). Thermally developing flow and heat transfer in rectangular microchannels of different aspect ratios. *International Journal of Heat and Mass Transfer 49*(17-18), 3060–3067.

Lee, P., S. Garimella, and D. Liu (2005). Investigation of heat transfer in rectangular microchannels. *International Journal of Heat and Mass Transfer 48*(9), 1688–1704.

Peng, X. and G. Peterson (1996). Convective heat transfer and flow friction for water flow in microchannel structures. *International Journal of Heat and Mass Transfer 39*(12), 2599–2608.

Qu, W. and I. Mudawar (2002). Experimental and numerical study of pressure drop and heat transfer in a single-phase micro-channel heat sink. *International Journal of Heat and Mass Transfer 45*(12), 2549–2565.

Shah, R. K. and A. L. London (1978). *Laminar flow forced convection in ducts : a source book for compact heat exchanger analytical data*. New York: Academic Press. ID: 4552273.

White, F. M. (2006). *Viscous fluid flow : (by) frank M. White.* (3rd ed.). New York: Mcgraw-Hill. ID: 301720193.

Investigation of hydro-dynamically and thermally developing flow distribution with optical measurements on a small width heat sink

LARS KUUR
Department of Energy Technology
Aalborg University

lkuur07 @student.aau.dk

***Abstract*—Experiments have been conducted on a heat sink with rectangular 2.35 mm width and 7 mm deep channels. The water flow field and temperature distribution have been investigated non intrusive with Particle Image Velocimetry (PIV) and Planar Laser Induced Fluorescence (PLIF), respectively. The cold side was investigated and a pseudo constant wall temperature was set on the hot side. The experiment was also equiped with thermocouples on inlets and outlets and flow meters. The flow was always laminar with Reynolds number ranging from $200 < Re < 1200$. The observed boundary layer development agrees well with classic expectations.**

I. INTRODUCTION

THE development of heated flows in the laminar regime is one of the fundamental problems in fluid mechanics. In an academic sense, it poses a problem easy to comprehend but difficult to master, involving many aspect while still, at least for the circular tubes and parallel plates, allowing for good analytical solutions White (2006). Despite decades of research and development of stronger computational powers there is still a lag of good correlations, correlations that will help chose the best design. Best as in not just the highest heat transfer coefficient but with the lowest pressure gradient required, the right temperature distribution and able to satisfy other non fluid mechanical demands (geometric constraints, weight, cost, lifetime). In another paper from this series (Kuur, 2011b), it is discussed how the microchannel design is especially critical. In the state of the art design methodologies, the aim is at an optimum solution by setting, among others, pressure loss as either a constraint or solving the problem as a multidimensional problem where the thermal resistance and pressure loss is minimised. A good example is the Thermal Electric Generator (TEG) which harvest the waste heat to generate small amounts of power which accumulates to a significant saving over time. The key thing to notice is that such designs must be evaluated on a system scale, the nature of the TEG means that increasing the heat transfer coefficient may give a very little change in overall power extraction, but a very big change in losses for thermal management. Although there has been a movement towards using CFD code coupled with an optimisation algorithm, such as Foli et al. (2006), the vast majority of suggested methods are still based on analytical derived expressions and fitted correlations. Lee et al. (2005) showed that many authors seems to arrive at significant deviations from what is considered a macro scale approach, but where Lee et al. (2005) argues that this could be because of the simplifications made for the developing zones.

One way of investigating this, is with numerical calculations. One example of rectangular channels with laminar flow and among others constant wall temperature, is by Lee and Garimella (2006) who find good agreement with the experimental results of other earlier experiments and with the correlations by Shah and London (1978). Lee and Garimella (2006) deviates from the experiment herein, in the sense that they use fully hydro-dynamically developed flow and that the boundary condition is applied at all four sides, no fins or isolating top plate. The most significant numerical deviations from experiments, are seen in the early developing zone.

The open data available from experiments is mostly obtained with one experimental concept, a number of thermocouples along the side the channel and flow and pressure sensors. Some works have performed μPIV to investigate the transition from laminar to turbulent, one of the areas where the micro-scale effects are said to come into play. Santiago et al. (1998) discusses the actual build and operation of such a device, Sharp and Adrian (2004) and later Li and Olsen (2006) both performs measurements in the transitional regime where the first can be considered as a paradigm shift by showing with a very broad yet thorough μPIV experiment that no discrepancies exists between macroscopic correlations and μ sized microchannels. Proving the value of such direct measurement equipment.

Despite the significant effort spent in investigations, the developing flow in channels are still mostly investigated indirectly. In this paper it will be investigated with PIV and PLIF. The μPIV differs from PIV in that PIV uses a laser sheet perpendicular to the camera view, μPIV uses a one way mirror and optics to project the sheet from the same direction as the camera view.

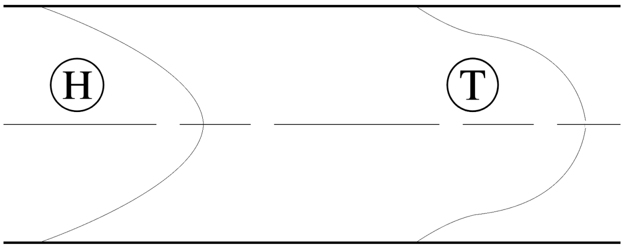

Figure 1. A comparison of the fully developed laminar thermal profile with boundary conditions for constant heat flux and constant temperature. With inspiration from Kays et al. (2007).

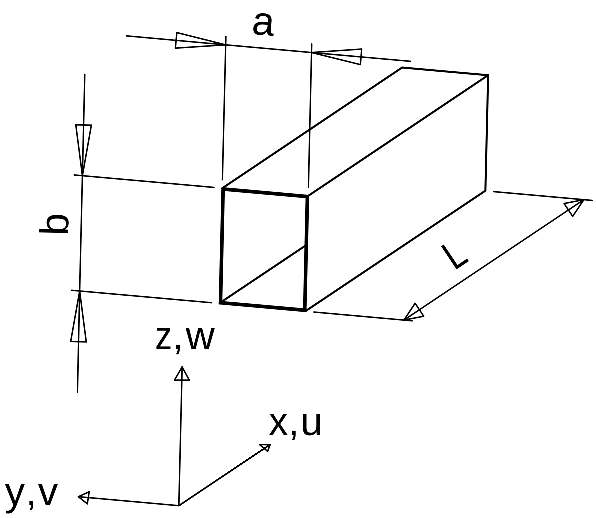

Figure 2. An example figure of the annotation used, it is preferable to use the Cartesian coordinate system although some of the simplifications from the tube can no longer be made.

II. Heated flows in a channel

In this section, and the following, we mainly adopt methods and approaches from Kays et al. (2007) and White (2006). Kays et al. (2007) defines two boundary conditions as H and T, constant heat flux and constant wall temperature, respectively. In the experiment at hand we operate with a quasi T condition[1]. When fully developed flow it can be shown that the profile of the two differs as shown in figure 1.

When describing the thermal properties of the fluid we can use the dimensionless Nusselt. Given as:

$$Nu = \frac{d_h h}{k} \tag{1}$$

Where

$$d_h = 4\frac{\textit{flow area}}{\textit{wetted perimeter}} = 4\frac{a \cdot b}{2a + 2b} \tag{2}$$

For reference, the annotations used can be seen in figure 2. For H it can be shown that in the rectangular channel the Nusselt number will be from 3.61 to 8.235 and for boundary condition T from 2.98 to 7.54, that is the two extremes, first is a square channel and last is two flat plates[2]. These numbers are found from numerical solutions of a simplified version of the energy equation, it is given as equation 3.

$$u\frac{\delta^2 T}{\delta x} = \alpha \nabla^2 T = \alpha \left(\frac{\delta^2 T}{\delta y^2} + \frac{\delta^2 T}{\delta z^2} \right) \tag{3}$$

Now using the momentum equation to derive an expression for u, it is seen that with the T[3] boundary condition this will be a mixed boundary value problem. The boundary conditions written explicit will be:

$$T\big|_{z,y@surface} = T_{surface} \tag{4}$$

$$\left(\frac{\delta T}{\delta z} + \frac{\delta T}{\delta y} \right)\bigg|_{x,y@center} = 0 \tag{5}$$

The pseudo coordinates given in equation 8 should be understood as the temperature is constant at the wall surface interface and that in the centre of the channel the symmetry gives zero temperature change in either z or y direction. The symmetry and the effect of the constant wall temperature can be seen in 3 from Lyczkowski et al. (1982). It is chosen to show a channel with only three heating walls as that is closer to what is done in this experiment. It should be obvious that the boundary conditions are still valid.

One major assumption for all this, is that no heat is conducted in the x direction (axial), it must only be transported by fluid movement, this is shortly discussed in the next section.

A. Inlet conditions.

The inlet conditions are different as part of the stream will still be free stream temperature, unaffected by whatever conditions at the wall. The hydrodynamical developing flow in the inlet of a channel is shown in figure 4

The thermal profile is much the same. But the properties of water ($4 < Pr < 7$) means that the hydrodynamical flow develops much faster then the thermal, and that in the developing zone the boundary layer will gradually build up but only at slow velocities will the diffusion og heat change the core flows temperature. This is shown in figure 5.

The problem as we approach it, was in it's simplest form considered by Graetz in 1883, the problem type is named hereafter.

The energy equation is reduced with the assumption of no axial heat conduction and no dissipation. White (2006) considers it negligible without debate, Kays et al. (2007) suggests that the $Pr \cdot Re > 10...100$ must be satisfied, where 100 means it is completely negligible. In this experiment this

[1]The validity of this condition is further described in Kuur (2011a)

[2]The difference between the two can intuitively be understood as that the flow progress along the channel length its temperature increases and the ΔT decreases. With the constant heat flux (and with the assumption of constant properties) the wall will heat to maintain the temperature difference and heat flux, so ΔT is constant for H and changing for T.

[3]Or with H boundary conditions as it is the same used

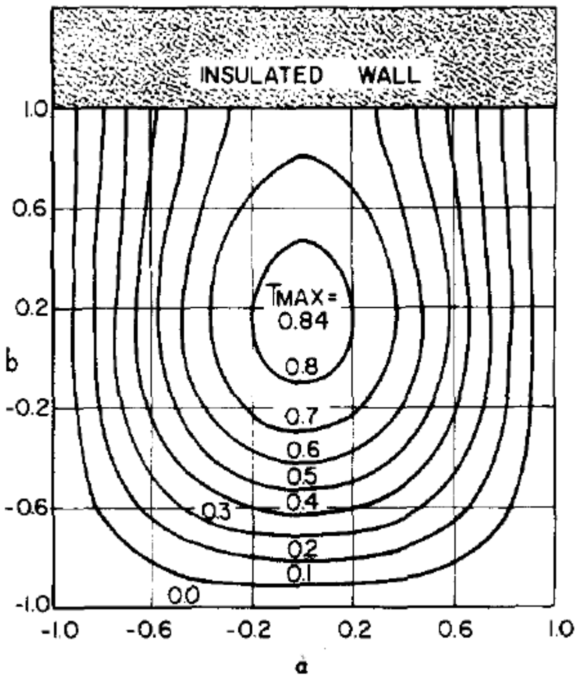

Figure 3. The contour lines given for the constant wall temperature, the centre symmetry gives the zero gradient, from Lyczkowski et al. (1982).

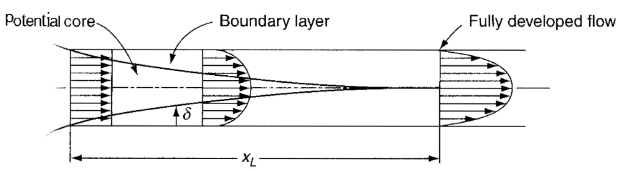

Figure 4. The developing flow, at some point it will become a Pousille flow with the characteristic parabolic profile, from White (2006).

number is never less than 500.

The concept of the Graetz problem, is to consider the flow exposed to a sudden change in wall temperature, and then applying a desired velocity profile through the axial transport term. As was shown in equation 3. The boundary conditions will become:

$$T\Big|_{z,y,x<0@surface} = T_{flow} \tag{6}$$

$$T\Big|_{z,y,x>0@surface} = T_{surface} \tag{7}$$

$$\left(\frac{\delta T}{\delta z} + \frac{\delta T}{\delta y}\right)\Bigg|_{x,y@center} = 0 \tag{8}$$

It can be seen form the first two, that before the channel inlet ($x > 0$) the flow will be exposed to it's own temperature. After the channel it is exposed to the constant wall temperature. White (2006) suggests three approached for what boundary conditions can be applied. The simplest is slug form, the second is Pousille flow (fully developed) and the last is to use an expression that describes the flow development. The last will make the problem significantly harder to solve. Kays et al. (2007) argues that if the Prandtl number is 5 or above

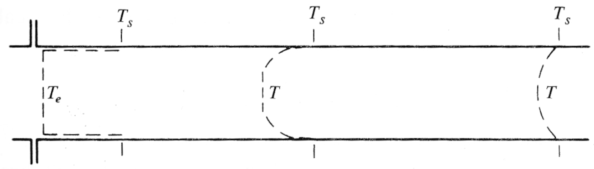

Figure 5. The thermally developing flow, in this case a flow being heated since the front is leaning backward, from Kays et al. (2007).

the hydrodynamic flow will develop so much slower then the thermal, so it can be assumed fully developed. As will be shown this holds true for this experiment although the Prandtl number is slightly under for some studies.

With the definition of some helping functions we can approach the Graetz problem:

$$\Theta = \frac{T_s - T}{T_s - T_e} \tag{9}$$

$$\Theta_m(x^+) = \frac{T_s - T_m}{T_s - T_e} \tag{10}$$

$$y^+ = \frac{y}{y_s} \tag{11}$$

$$u^+ = \frac{u}{V} \tag{12}$$

$$x^+ = \frac{2(x/D_h}{RePr} \tag{13}$$

With some algebraic work it can then be shown that [4]:

$$Nu_x = \frac{2y_s h_x}{k} = \frac{2y_s \dot{q}''(x^+)}{k(T_s - T_e)\Theta_m(x^+)} = \frac{-2}{\Theta_m}\left(\frac{\delta\Theta}{\delta y^+}\right)_{y^+=1} \tag{14}$$

Now consider the last term of equation 14, it would seem that with a number of temperatures and the changes we can determine the local Nusselt number. This is something we will use with the PLIF measurements.

The alternative to this, is to consider the second the terms in equation 14. With some effort this can be recognised as involving the classic "Newton law of cooling" approach:

$$\dot{q} = h \cdot A_s \cdot (T_s - T_m) \tag{15}$$

Substituting the various dimensionless terms it should be recognised that these are identical when:

$$\dot{q}'' = k\frac{T_s - T_e}{r_s} \cdot \left(\frac{\delta\Theta}{\delta y^+}\right)_{y^+=1} \tag{16}$$

But there is a not so elegant way of determining $\dot{q}''$. By discretising the channel in the flow direction and making an energy balance across the cell, we see:

$$\dot{q}_x'' = \frac{c_p \dot{m}(T_{m,x+1} - T_{m,x-1})}{A_{s,x}} \tag{17}$$

[4]Notice this is rewritten from the derivation for a circular tube.

This is also referred to as an integral approach.

For the later, it is assumed that the temperature profile do not change with z, obviously, and with reference to figure 3 this is wrong but for the accuracy that can be obtained in the experiment it is an acceptable assumption. For the same equation the area is rewritten for our channel rather then for a tube. The first term is meant for a tube but since we will experimentally determine the $\left(\frac{\delta\Theta}{\delta y^+}\right)$ term it is of less importance. It does still play a role however, the expression uses a consideration for the circumference in the derivation from the energy equation, this will be invalid for the rectangular duct. It is difficult to come up with a proper analytic alternative. Since the profile is, in this experiment, only determined for one height it will be just as much an assumption to start working with this as a two flat plates. One method may be to fit the distance (y) to the hydraulics diameter (D_h). This would require some sort of enforcement on the data set and still assume that the observed thermal condition is axial symmetric - But it is expected that the fins have variation in temperature, and that the top plate is isolated. Using either would require new experiments to validate the method. It is chosen to use the equation in it's current form since the alternatives has equal downsides.

For which method is the best, the later requires that the energy balance can be set across a section, and that requires that the average section temperature is precisely determined relative to the bordering cells. But the PLIF system allows determination of the 2d thermal profile, when using this discrete approach the quality of the information is degraded to just 1d. This is not the case when using the gradient based method.

One way not to degrade the information is to not just take the average of the cross section temperature, but rather integrate across, as:

$$\dot{q}_x = \int_{y_w}^{y_c} u_y \frac{\delta T}{\delta x} \rho c_p Z dy \tag{18}$$

This equation only holds for flows that are only moving in the x direction (laminar), with the assumption of no change in the z direction[5]. Recalling the energy equation (equation 3), and that the transport term is then the same as the one in equation 18, then it should also be recognised that this term can be filled with measurements of the actual velocity profile - As done with PIV.

III. Experiment and the setup

The experimental setup can be categorised into three subsystems:

- Thermal control system
- Indirect measuring equipment
- Optical measurement equipment

The second, indirect measuring equipment, and the result of an analysis of just those results, are presented in Kuur

[5]But can easily be extended

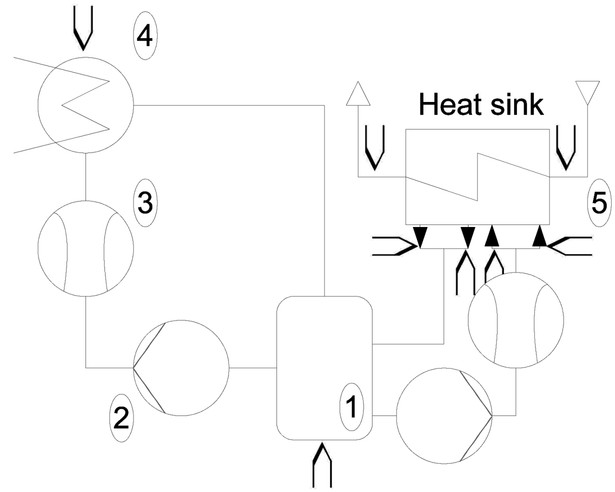

Figure 6. The hot side diagram, 1 is the basin where the water from the kettle (4) is mixed to in to get the desired temperature.

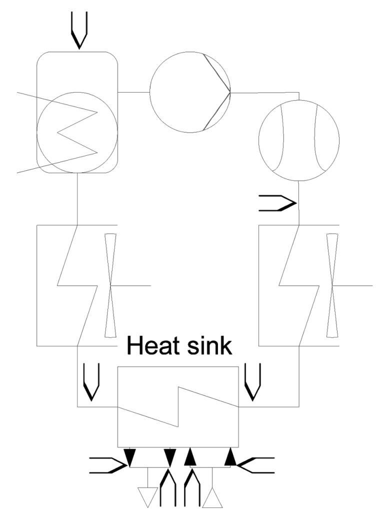

Figure 7. The cold side diagram, much cooling is needed to maintain a big temperature difference between hot and cold.

(2011a). The indirect measurement equipment is also used for the optical measurement equipment for performing the calibration and the thermal control system relies on the inputs to control the temperatures with a program made in LabView$^{\mathrm{TM}}$. The thermal control system manages that the temperatures stays constant when desired. The optical measurement equipment is the Dantec$^{\mathrm{TM}}$PIV with PLIF add-on system.

The measuring equipment and points of measuring will be shown in this article but the treatment of uncertainties will not be repeated. In figure 6 the hot side system is shown.

And in figure 7 the cold side is shown, this is also the side that is observed. The reason why the cold bath is heated (upper left side in the diagram) is that a wide range of temperatures must be observed when calibrating. It is faster to heat directly on the fluid then heating by heat exchanging with the hot side.

For the optical measurement the setup is made with two acrylic plates, one perpendicular to the flow and one normal

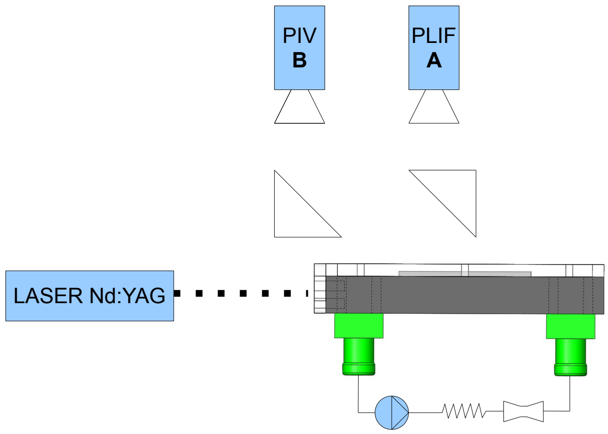

Figure 8. The laser sheet illuminates the flow, the round polyamid seeding particles reflects the green light which is filtered and reflected to camera B. The Rhodamin absorbs the light and re-emits at a lower frequency, this orange light is only seen by the A camera.

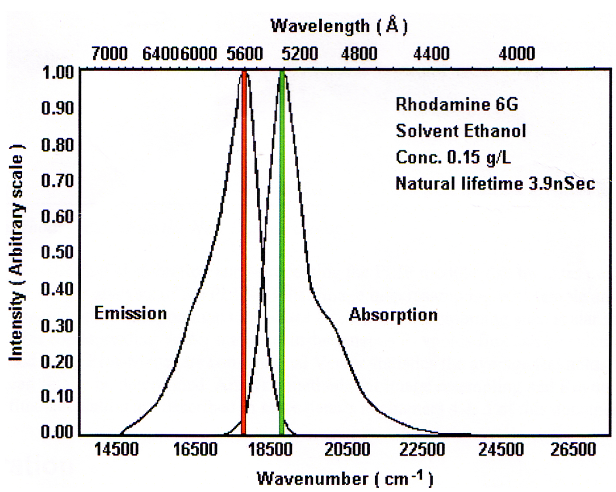

Figure 9. The emission and absorption of Rhodamine. It can be seen how it is an excellent solution for ND:Yag lasers (green light), from Dantec (2001).

to the flow. The diagram drawing in figure 8 shows this.

The camera A is equipped with a filter so that it only sees light in the red/orange spectrum. When a Rhodamin particle is hit by a green photon it absorbs this, becomes elevated in its quantum state and eventually falls down to re-emit the photon with a lower frequency (orange spectrum). The chance of this happening is among other dependent on the fluid temperature. With other properties constant (especially concentration) the intensity of the light will then depend only on temperature. In figure 9 the emission and absorption span are shown.

The camera B also has a filter so that it only sees the green light, when one of the round polyamid seeding particles are illuminated they scatter the light and camera B observes the movement of every particle over a very short timeframe. At each recording two pulses occur with 3000 μs time between, each pulse has a duration of 0.01 μs.

The equipment used are:

- 2x HiSense Type 13 cameras with gain 4, 12 bit grey scale, 1280x1024.
- 2x Micro-Nikkor 60mm lenses
- NewWave Gemini laser emitting at 532 nm wavelength (Nd:YAG laser)

Only the PIV system needs the second pulse. The pulses are not identical because it is two different lasers that makes the two burst, and the light exposure is different for the first and second burst. This makes it no good for the PLIF system. For the PIV system, the pixel to mm ratio is 36.59, this makes one channel almost 86 pixels in the cross sectional direction. It was chosen to first use 20 μm particles, later 5 μm was used, both are discussed later. The big particles used sets a limit to the amount of seeding. With 20μm one particle is 0.85 % of the channel width. But since it is expected that this will be laminar flow the seeding does not need to be as intensive as if we wanted to capture eddies.

It can readily be shown that: $V \cdot Pix/mm\Delta t = \Delta s$ and that the distance moved Δs is recommended to be $1/4$ of the investigation area, in this case 32 in x direction. Then this will be 8 pixels. We want to capture flow velocities between 0.05 to 0.15 and this will be 5 to 16 pixels movement. That span is acceptable and should give good results.

In figure 10 two photos from the experiment are shown. It is the system from distance and a close up that shows the laser sheet into the setup.

A. *Calibration of PLIF*

Before measurements can be made with PLIF, it must be calibrated. This is done by circulating water at constant temperature so there is no temperature change. The intensity of the flow can then be registered for that specific temperature. Repeating this for a range of temperatures allows for a linear fit to be made. This fit is later used to find the actual temperature when the flow is heated. If this is done for the entire geometry at once and one single calibration is made,then for this experiment the linear fit becomes as in 11.

This is not a good method in this case. First of all, the channel walls must be filtered somehow as they obviously can not be expected to do as the fluid. Second, as can be seen in figure 12, the shading from the channels and the results of reflections makes some areas more exposed.

The software that handles the picture acquisition, does have a masking tool and calibration algorithms. But it was chosen to do the calibration for every pixel with a moving average smoothing in Matlab$^{\mathrm{TM}}$, this allows for a more open approach to the dataset and methods applied. The averaging is simply:

$$\overline{I}(x,y) = \frac{1}{9} \sum_{n=-1}^{+1} \sum_{m=-1}^{+1} I_{x_n,y_m} \tag{19}$$

With 1024x1280 pixels this must be evaluated for 1310720 points. The dataset can overall be considered as a 3 dimensional matrix, I(x,y,k). The third dimension holds each of the different calibrations, 9 in this case. Alongside is the associated temperature vector T(k), obviously k takes the size of 9. The dataset is in this case 11.8×10^6 points[6]. Using least

[6]The point being, that optical flow measurements is one of the few types of experiments where the amounts of data can become a computational challenge

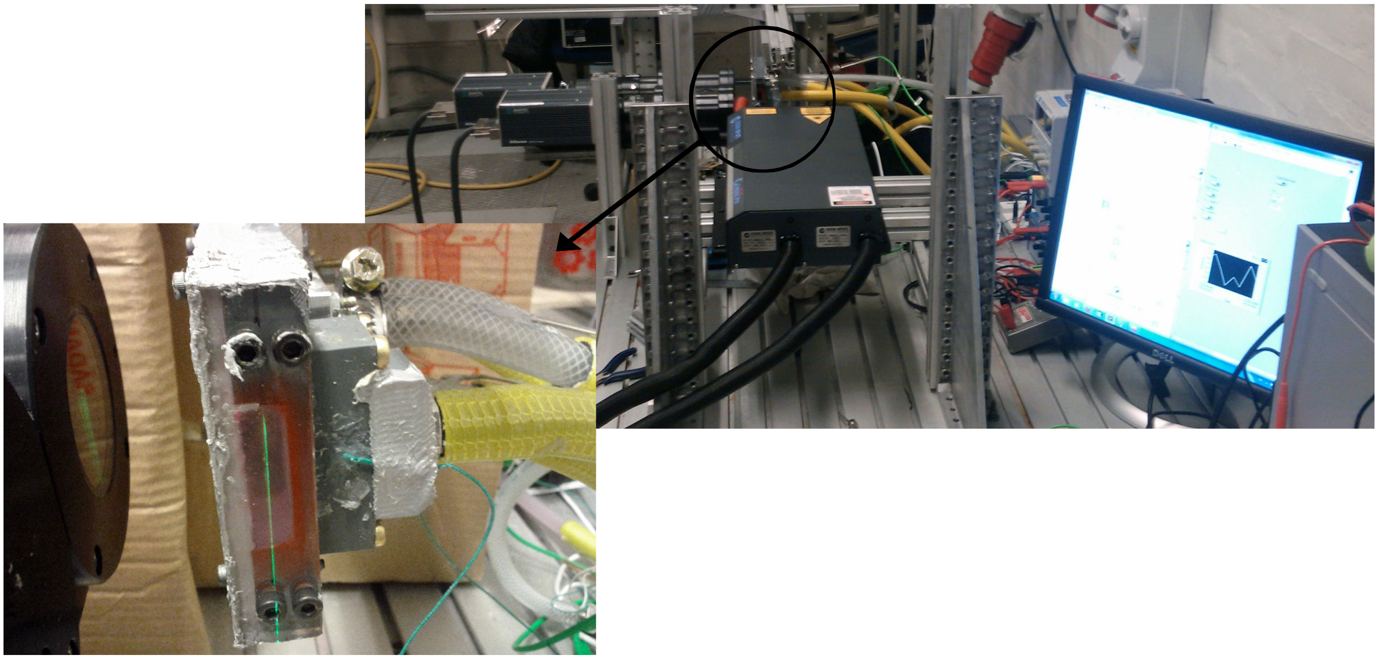

Figure 10. Photos from the actual setup, with a close-up of the laser sheet (at low intensity) taken during the alignment work (the sheet is slightly tilted in the picture).

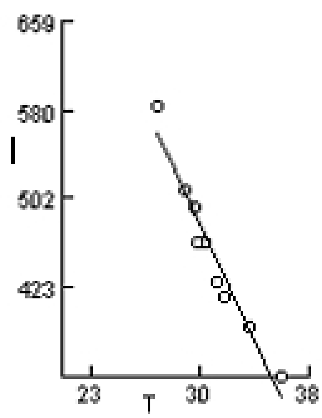

Figure 11. Linear fit to the overall average intensity and temperature with the channels masked so they do not interfere

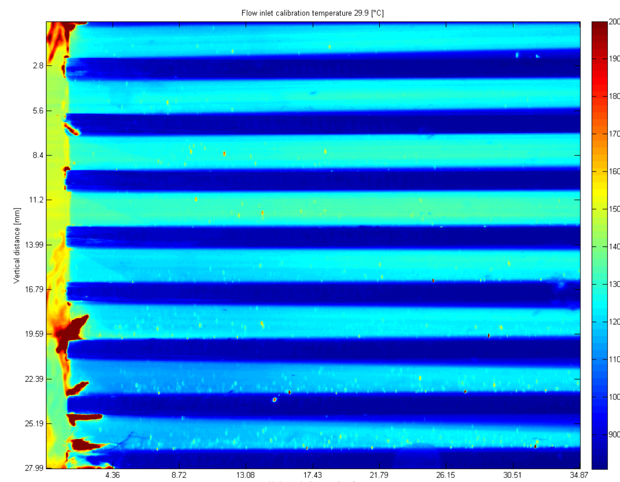

Figure 12. One calibration point composed of 50 images, with intensity shown as colour, an upper limit at 2000 is set. Notice that the shades seems to tighten the channels towards the end

squares method we find the coefficients for a fit at every point, using the Matlab function annotation[7]

$$m_{x(n),y(n)} = [I_{x(n),y(n),k}, 1] \setminus T_k \tag{20}$$

That will give two coefficients for every pixel in the picture. Transferring this into a temperature for an actual measurement is easily done with $m_{x,y} \cdot [I_{x,y}, 1] = T_{x,y}$

The result is that no masking is done, but ideally the shadows should not change from one calibration or measurement to another, and assuming the shaded areas are still exposed to some light it will still be temperature dependent and should emit dependent of temperature. How this holds up can be seen in figure 13

It can be seen that in the lower inlet some movement are happening. This can partly be because of how the light is scattered, it is focused on the third channel from the top. Some shading effects are also still seen. But in general the result is good, even though the temperature difference is just 3 $°C$ it is easy to tell the three apart.

IV. Results

In figure 14 the result for one channel is shown.

From this we find the thermal profile as in figure 15

[7]mldivide, or \ is actually not least squares method but a much faster version that exploits some matrix calculus about the under-determined problem we face mathworks (2009)

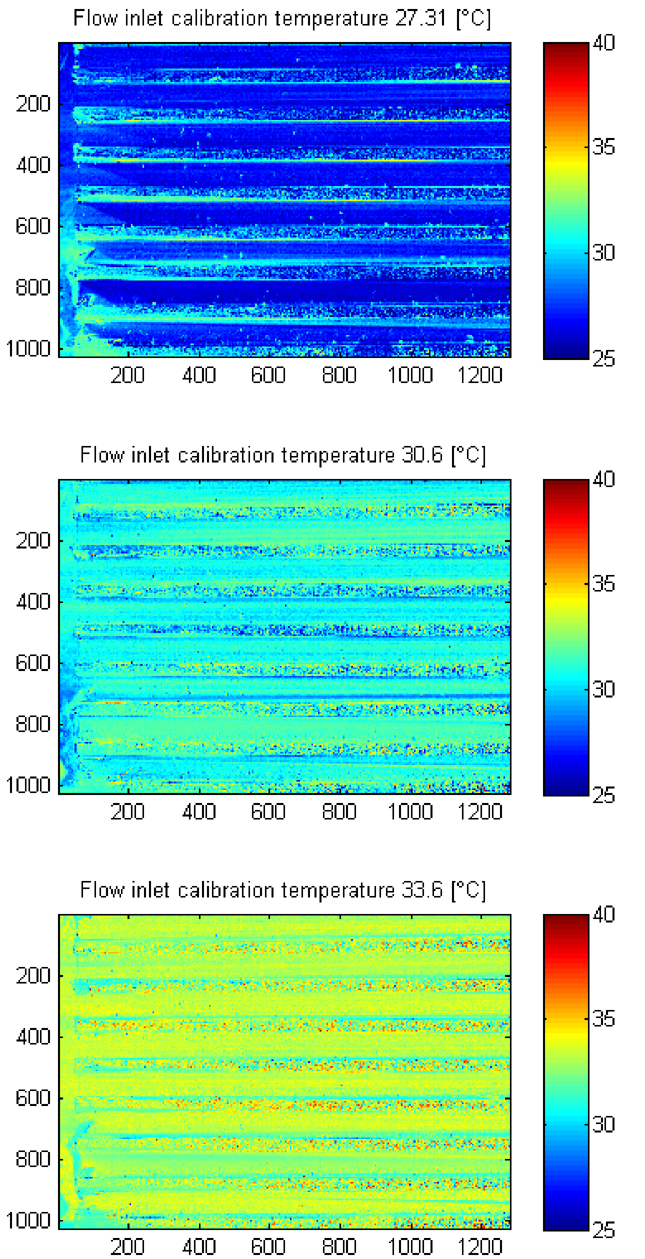

Figure 13. Three channels with the calibration applied. Ideally they should each be just one single colour accordingly to their temperature.

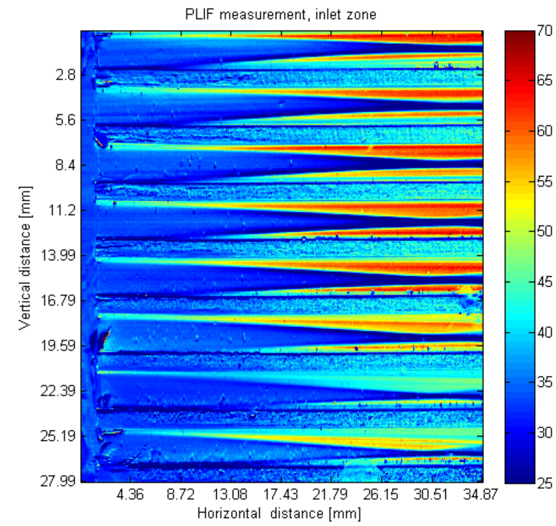

Figure 14. One example PLIF measurement, limited to $25 < T < 70°C$.

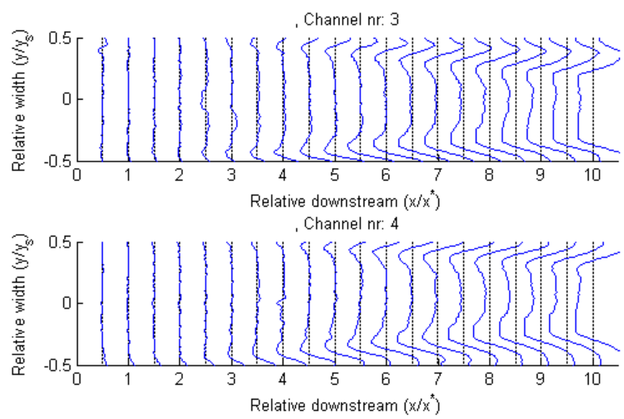

Figure 15. Dimensionless thermal profile plots.

The profiles are dimensionless by width and length, notice that x^* is not the fully developed length, it is just the entire investigated length.

The thermal profiles are calculated relative to the non dimensional temperature, as previously shown:

$$\Theta = \frac{T_s - T}{T_s - T_e} \tag{21}$$

$$\Theta_m(x^+) = \frac{T_s - T_m}{T_s - T_e} \tag{22}$$

Mind that the dotted line are taken as the mean line for each profile (Θ_m), not the wall temperature.

It can be seen that the thermal profiles expect much as expected. There is however some discrepancies:

- At the wall the temperature starts falling again.
- The core flow bends gets hotter in the centre.
- The flow is not entirely symmetrical

These problems are all expected to be caused by the PLIF methods. And are not reflections of what is actually happening. The problem with the fall in wall temperature can be explained by how PLIF works, when the intensity is high, the temperature is low. The direct incoming laser sheet is shattered the further downstream, instead an amount of reflections are present. These reflections are so intensive at the walls that they appear as a lower temperature. The reason why this is not solved with the calibration is that the concentration or setup it self may shift slightly doing the experiment. More work will be needed to determine a more exact cause.

The problem with the core flow getting first very cold, and then hot again, is an effect from taking the mean of the profile for comparison. In an absolute sense, the core flow gets colder downstream, as can be seen in figure 15, it is more than 5 $°C$ colder then the inlet temperature. This is obviously wrong and against the first law of thermodynamics. The peak of the forward core stream parabola is the right temperature. It seems that this happens with the slow flow velocities, other measurements with higher flow velocities and less developed boundary layers do not have this effect. Not enough is known about this.

Lag of symmetry can be attributed to the inlet conditions that are not uniform plug flow.

Finding the gradient $\left(\frac{\delta\Theta}{\delta y^+}\right)$ was a problem because the temperature problem close to the wall. Since the temperature would seem to be higher just a few cells outside the wall, the gradient evaluated at $y^+ = 1$ will be positive and not reflect the actual boundary layer. A number of methods was tried to remedy this, one method was to create a scaled thermal profile by:

$$T_{scale,y^+} = (T_{y^+} - T_{min})\frac{T_w - T_e}{T_{y^+=@T_{y,max}} - T_{min}} + T_e \quad (23)$$

Which is a scaling of the temperature, the fraction makes it so that the profile is kept from highest to lowest, but the profile is linearly modified to fit the upper and lower limits of T_w and T_e. But the method is also very sensitive to T_{min} and T_{max}, small variations can be very determining for the solution. The method also means that points defined after T_{max} and before T_{min} will get the set upper and lower temperature. Such averaging destroys information contained in the profile. It is difficult to tell if it is the points suggested for averaging, or the basis for the averaging (T_{min}, T_{max}) that is not real.

A less elegant way of finding the gradient was eventually used. Consider again figure 15 and see that the dotted mid line in the plots represents some centre. Now consider that an approximation can be made from the peak of the temperature profile to that line. This does not capture 2nd degree information, but it will capture how the boundary layer changes.

With the gradient determined the Nu_x value can be found. This is shown in figure 16.

It should be noticed that the flow is not expected to be fully developed before $x^+ >> 0.2$. But the absolute value is very low, it is believed this is because of the gradient not being steep enough. It is a problem that the temperature of the boundary layer indicates nearly wall temperature, while other parts of the core temperature are below the inlet temperature. Since this method is so dependent on the wall conditions this area should be trustworthy for it to work. It would be interesting to know if this is a scaling/calibration issue or if this is some more fundamental flaw. So we considered the mean flow temperature in figure 17

A rapid increase in temperature, this is not far from the 5 $^{\circ}C$ that is the expected as total temperature change, but the channel is only 34 of the 57 mm downstream, so the temperature readout is overall probably too high, that indicates the concentration has been reduced (Rhodamin tends to deposit in the auxiliary heat-exchangers)

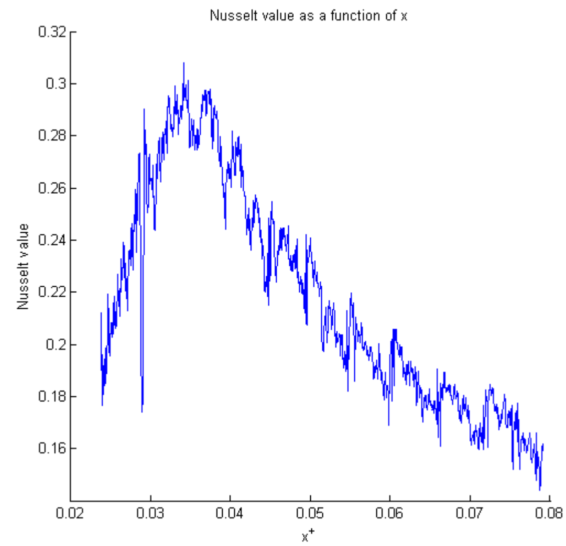

Figure 16. Nusselt values along x with the gradient based method, the function is behaving as expected, but in an absolute sense the value is wrong with about 200%

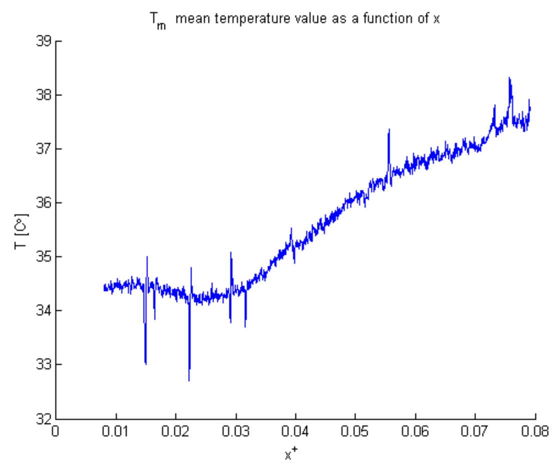

Figure 17. Mean temperature development of the investigated section.

At this point the discrete scheme method was tried. The data set was filtered with a reduction of cells by a factor of 5 and multiple times moving average with one neighbouring cell, that is a very steep averaging but necessary because of the noise when attempting to do point pr point balance. The result is shown in figure 18

The profile is no where near what is expected, it could be argued that in the beginning there is some resemblance of the expected profile, but not towards the ends. This shows that the problem with reflections and oddly behaving core flows towards the end, introduces uncertainties of such magnitudes that an discrete scheme of this kind is not possible with this quality data set.

The values, in an absolute sense, are above what is expected, Kays et al. (2007) gives that at $x^+ = 0.01$ the value for the geometry in question should be about 6 and drop to 5 at 0.02. In the description of the theory it was discussed how the mass flow $(\dot{m})$ should be resolved into a u profile and each cell

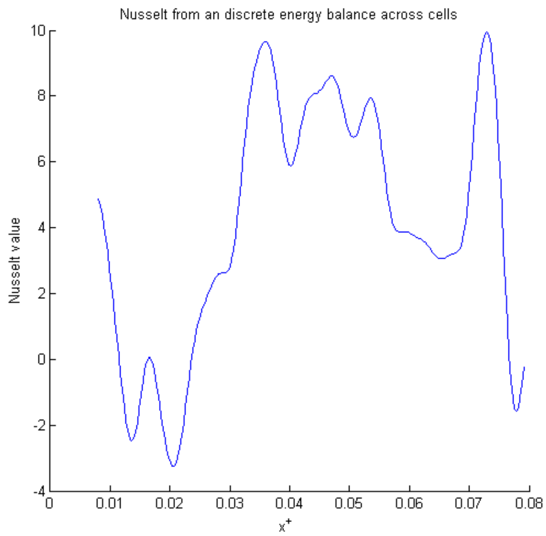

Figure 18. The Nusselt number when using an energy balance in a discrete sense, also called an integral method

could be evaluated in a 2d sense.

That would improve the quality since:

$$\frac{\delta}{\delta y^+}\left(u \cdot \frac{\delta \Theta}{\delta x^+}\right) \neq const \qquad (24)$$

- Or in other words, both the velocity is not uniform (plugged flow), and the change in hydro-dynamically and thermal conditions in the inlet area is not constant, the approach used to find figure 18 assumes both these.

A final comment is that the difference between the two methods is how $\dot{q}''$ is determined. The first uses the observed actual boundary layer information inserted into parts of the Navier-Stokes (energy eq) with the fully developed pousille flow parabolla, while the second method considers the change in the energy balance that will occur as a result of the first mentioned effects, but with a number of assumptions. The results are as seen very different.

A. PIV

The PIV measurements that was also determined has not been discussed much up to this point. A problem with the methods meant that no useful measurements was made for the treated PLIF example. However a similar mass flow case is treated here. PIV is interesting for a number of reasons, for the heat balance, the most prominent is that the energy balance method presented above can be improved with the information of the flow velocity (u). That will allow a 2d discretisation scheme.

In figure 19 the results from one case is shown.

It can be seen that the velocity nearly immediately takes up a form closely resembling the Pousille distribution. But not entirely, as will also be expected that the core flow keeps accelerating as the flow is not yet fully developed at the outlet of this test section. This change is however negligible. In the lowest of the three images an actual photo is shown from the experiment result. It can be seen (before the heat sink) that the seeding is high. But inside the channels the amount of light makes it look like less than what it actually is. Looking at the end of the channel, around 30 mm, it can be seen how the shading means no particles reflects light at the walls. This is also a good explanation why the inner boundary layer appears to be so hot in the PLIF analysis. It was theorised earlier that the calibration would deal with this kind of problem, if just a little light escaped from the area then it would still behave temperature dependent. But this PIV experiment shows

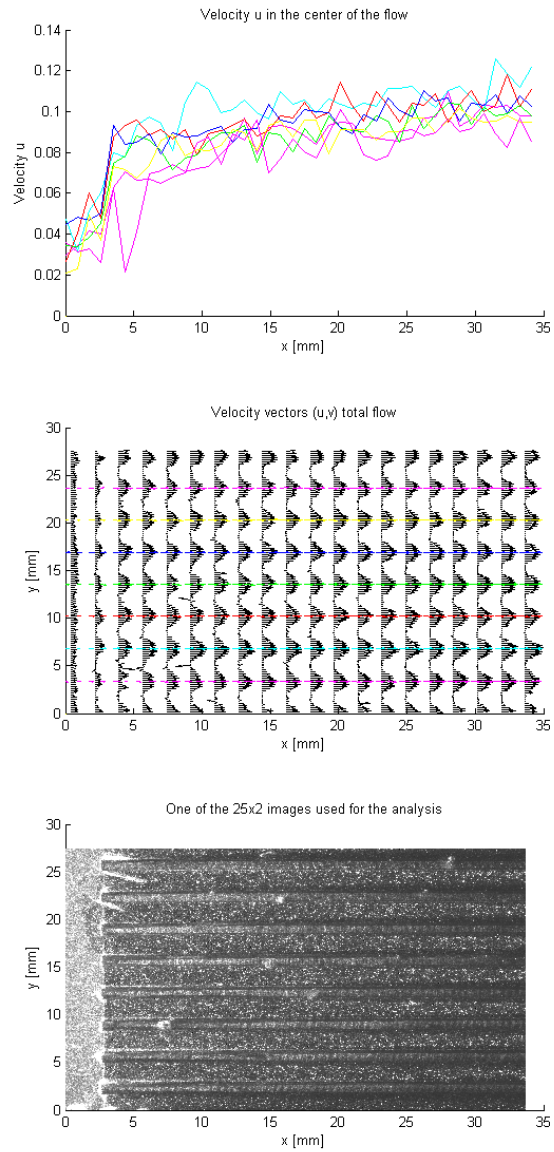

Figure 19. First picture shows the centre flow velocity in the x direction; The middle image shows the vector plot and last shows one of the PIV images used to calculate the vector map. Colour codes are used to show channel to channel

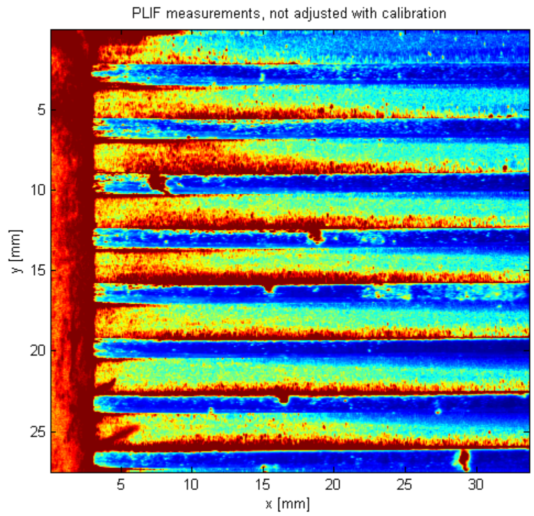

Figure 20. The simultaneous PLIF measurements in an nu-calibrated version, this can not be used for anything

that very close to no light escapes these regions. This does not invalidate the entire PLIF section, just shows that close to the wall at the ends of the channels, the laser sheet has problems illuminating the entire flow. It was attempted to do PLIF measurements on this same sample. The result is shown in figure 20

Even though figure 20 has not been adjusted with a calibration, it is very wrong already it it's current form. Calibration measurements was taken but they are equally distorted. It would seem that the PIV particles shades the PLIF particles and makes it very difficult to get accurate measurements. Any light emitted from a Rhodamin particle will still get reflected by a polyamid seeding particle. The seeding of the flow can then be reduced to help this problem. This was tried but more work and time should be dedicated for this. The preliminary attempts showed that even when seeding was kept at a level where the velocity plot could barely be resolved, the distortion for the PLIF was still too great and no good results was obtained.

One, at this point unaddressed issue, is the big particle side (0.86% of channel) . This was changed to investigate the effect of these. The test was to run the experiment with $5\mu m$ particles. This for several reasons, the most important being that the PLIF may be easier to observe with smaller particles. The downside is that the small particles easy cluster in the reservoir and heat exchangers, and are generally harder to trace. In figure 21 this is shown.

It stands out that the trends are the same as for the bigger particles. The smaller particles did not solve the problem with running PLIF and PIV at the same time. The PLIF data was still very much influenced.

V. Conclusion

An investigating of the flow in the inlet region of a heat exchanger has been presented. The theory for describing the

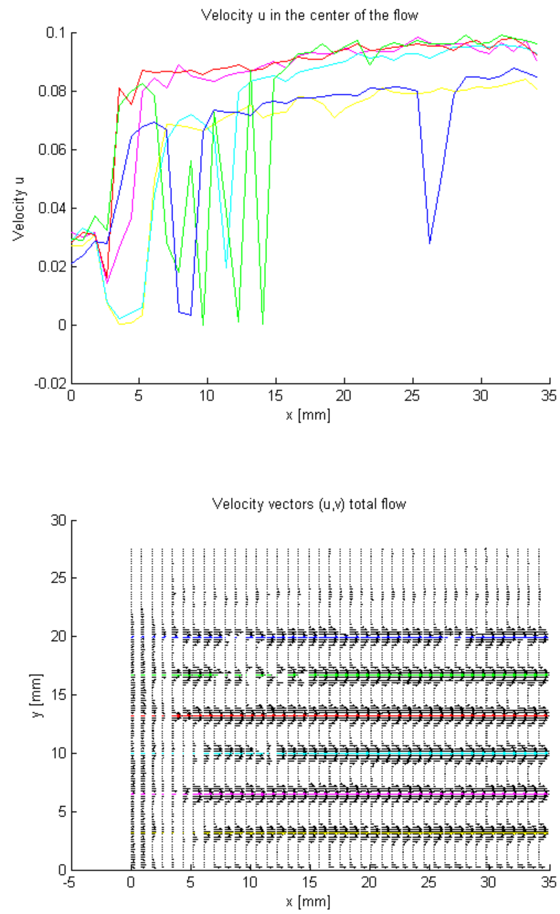

Figure 21. Result from running with $5\mu m$, it is more difficult to resolve the complete field.

inlet flow with focus on methods of direct determination of the Nusselt number discussed. Other authors who have made experiments have been discussed and it has been shown how the main issue is with the immediate inlet, the investigation focus has been on this part. A setup has been presented that uses a combined PIV/PLIF system and a laser sheet perpendicular to the view. It is shown that the thermal developing zone can be observed and a boundary and changes in the temperature can be observed which gives an indication of trends. It was investigated if the quality of this information was at a level where it could be used to tell about heat transfer coefficients and Nusselt numbers directly. Something that has received close to none attention in the limited literature. Several schemes was proposed, some with a significant amount of data correction. It must be concluded that even though the observations serves well as a visual concept of the boundary layer, it was in this experiment not possible to archive a level of quality that allows for direct readings of such numbers. A higher number of pixels in the channels and better illumination would be required to proceed with this. It was also investigated how the PIV and PLIF system could work together in this system. This kind of combination have to this authors knowledge never been tried in such small channel sizes. It was concluded that the PIV system did perform as expected, predicting the laminar flow very well. But a future prospect was that if the PIV and PLIF could work simultaneously this could also be used in the transitional/turbulent regime to determine thermal and momentum flux. But even with the much simpler laminar flow it proved very difficult to get good PLIF measurements. Despite many difficulties a thermal and hydro dynamically entry profile has been determined for various flows. This shows that despite it's many limitations this method does have potential as this allows for direct (visual) comparison with numerical CFD solutions.

References

Dantec (2001). Flowmanager add-on: Plif-module installation and user's guide.

Foli, K., T. Okabe, M. Olhofer, Y. Jin, and B. Sendhoff (2006). Optimization of micro heat exchanger: Cfd, analytical approach and multi-objective evolutionary algorithms. *International Journal of Heat and Mass Transfer 49*(5-6), 1090–1099.

Kays, W. M., M. E. Crawford, and B. Weigand (2007). *Convective heat and mass transfer*. Boston [u.a.]: McGraw-Hill. ID: 699686337.

Kuur, L. (2011a). Experimental study of a heat-sink.

Kuur, L. (2011b). Thermal management of a teg using an optimisation scheme for microchannels.

Lee, P. and S. Garimella (2006). Thermally developing flow and heat transfer in rectangular microchannels of different aspect ratios. *International Journal of Heat and Mass Transfer 49*(17-18), 3060–3067.

Lee, P., S. Garimella, and D. Liu (2005). Investigation of heat transfer in rectangular microchannels. *International Journal of Heat and Mass Transfer 48*(9), 1688–1704.

Li, H. and M. Olsen (2006). Micropiv measurements of turbulent flow in square microchannels with hydraulic diameters from 200 [mu] m to 640 [mu] m. *International journal of heat and fluid flow 27*(1), 123–134.

Lyczkowski, R., C. Solbrig, and D. Gidaspow (1982). Forced convection heat transfer in rectangular ducts–general case of wall resistances and peripheral conduction for ventilation cooling of nuclear waste repositories. *Nuclear Engineering and Design 67*(3), 357–378.

mathworks (2009). Matlab help file. Technical report.

Santiago, J. G., S. T. Wereley, C. D. Meinhart, D. J. Beebe, and R. J. Adrian (1998). A particle image velocimetry system for microfluidics. *Experiments in Fluids 25*, 316–319. 10.1007/s003480050235.

Shah, R. K. and A. L. London (1978). *Laminar flow forced convection in ducts : a source book for compact heat exchanger analytical data*. New York: Academic Press. ID: 4552273.

Sharp, K. and R. Adrian (2004). Transition from laminar to turbulent flow in liquid filled microtubes. *Experiments in fluids 36*(5), 741–747.

White, F. M. (2006). *Viscous fluid flow : (by) frank M. White.* (3rd ed.). New York: Mcgraw-Hill. ID: 301720193.

Conclusions and discussion

At this point the three papers has been presented. In this section the most important conclusions for each paper will be highlighted and some final overall conclusions and reflections presented.

A number of bullet conclusions is highlighted first of all:

- State of the art for TEG's and it's relation to heat sinks and microchannels in particulair
  - Know how and methods from Heat Sink design has a role to play in the creation of TEG systems, and as the TEG systems gets closer to a general commercial breakthrough this demand increases.
  - The TEG technology are still challenged by other technologies and the fundamental issue with low efficiency
  - Key players has identified thermal management as one of the pillars for a break through for TEG's.
  - It is seen that while not the case now, soon TEG's requires heat exchangers with performance like what microchannels can do.
- State of the art for designing microchannel heat sinks
  - Many of the optimisation schemes are build on very simplified correlations
  - In recent years many of the disputes regarding microscale phenomenas has been, alteast somewhat, settled, μPIV has played a significant role in this
  - Many authors now find good agreement with classic macro scale methods
  - Some more advanced correlations has been found, for the exotic combinations of phenomenas often encountered with microchannels, but significant deviations between each correlation is seen
  - Most experiments uses some sort of integral method for finding the flow properties
- Experiment on a mini channel (2.35mm width, 7mm deep
  - Using an integral method it was posibal to find the Nusselt number for the entire heat exchanger
  - With the quality of the current experiment it is not possible to determine an absolute local Nusselt number along the flow direction x.
  - PLIF and PIV together has issues with plastic particles from PIV that blocks and shatters the light for PLIF. More work are needed to make this combination work.
  - Getting the correct and constant exposure of light is difficult. It seems the PLIF results are very sensitive to even small changes.
  - The channels must be resolved into enough pixels to get a resolution that can be used. But a certain length of the channel must also be observed to actually see any temperature changes.
  - The visual impression of the boundary layer is good and the hydrodynamical profile is as expected.

As mentioned in the bullets it can concluded from the revieved litterature, that there is a lag of experiments that concerns it self with these more practical configurations. And the TEG will soon requires this kind of tailored solutions. While TEG was the only application reviewed there seems to be many posible situations where microchannels could benefit. At the moment much research is put into other microfluidic devices, such as cheap ways of producing micropumps. As this technology continues to mature there seems to be a potential for microchannels to compete with the big passive heat exchangers seen everywhere today.

For the experiment it is mentioned that the number of pixels observed is important. To get more cross sectional pixels per channel the camera must be moved closer, this will be a trade off between being close with high resolution of the channel, but only a small length, and vice versa. Many ways exists to solve this. As long as the flow is only steady state the camera can be transversed downstream. If the flow is not steadystate then a setup with more cameras could be used, then the cameras will overlap each others flowfield. Both solutions will further complicate the already complicated setup.

The inability to get good measurements with both PIV and PLIF is discouraging, but, although a subjective opinion of the author, it is posibal to get good results with more work, better controlled conditions, better calibration and better data treatment methods. Adjustments to the seeding and light exposure is definatly a part of the solution. But two types of seeding that influences each other and a laser intensity there is many unknowns. Add to this that the distance from the laser beam splitter to the heatsink, and at what height in the heatsink the laser sheet is projected, the future work needed is very significant. For the data treatment it was attempted to use knowledge about the flowfield to adjust the dataset, with some sucsess, with a good understanding of the expected phenomenas this can further be developed. Also with better calibration and possibly a calibration after the measurements the temperature could be better estimated. What can be archieved in this simple study with both PIV and PLIF measurements is limited as the flow is hydrodynamically developed to a degree where the change in profile is negligle compared to noise. But once the phenomenas and solutions to the problems are well described and understood this method can be extended to flow in the transitional and turbulet regime, and even more complex geometries. Being able to do so for small geometries is very attractive.

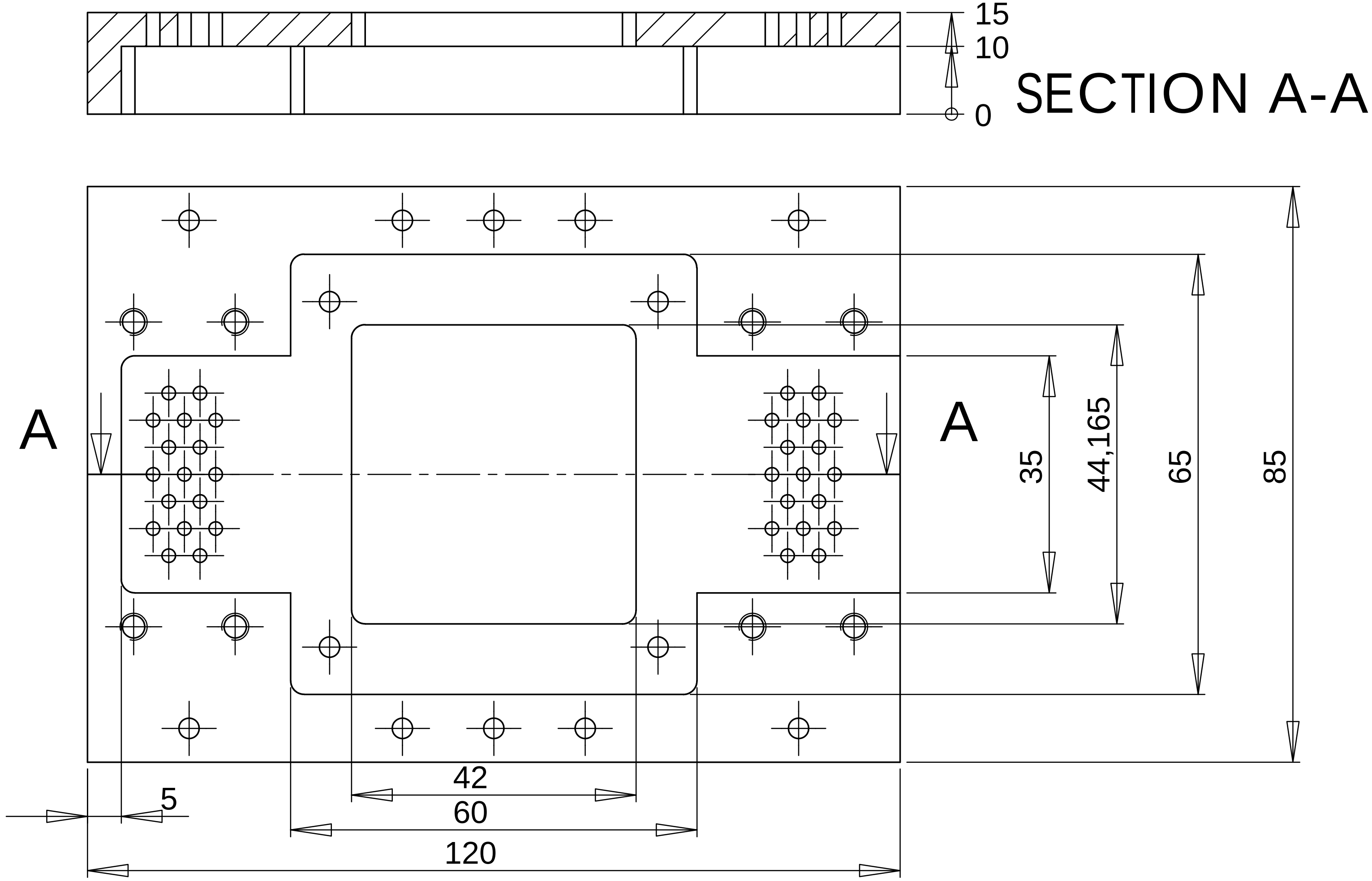

UNLESS OTHERWISE SPECIFIED:
DIMENSIONS ARE IN MILLIMETERS
SURFACE FINISH:
TOLERANCES:
LINEAR:
ANGULAR:

FINISH:

DEBUR AND BREAK SHARP EDGES

DO NOT SCALE DRAWING

REVISION

Cont: Lars Kuur - 26828419 (energi 10sem)

	NAME	SIGNATURE	DATE
DRAWN			
CHK'D			
APPV'D			
MFG			
Q.A			

TITLE:

Microhannel proj

MATERIAL:

Nylon eller tilsv plast

WEIGHT:

DWG NO.

MountingPlate

A4

SCALE:1:1

SHEET 2 OF 2